IMPI's 55TH ANNUAL MICROWAVE POWER SYMPOSIUM

(IMPI 55 VIRTUAL SYMPOSIUM)

2021 PROCEEDINGS

June 28-July 1, 2021

Virtual Symposium

ISSN 1070-0129

Presented by the
INTERNATIONAL MICROWAVE POWER INSTITUTE
PO Box 1140, Mechanicsville, VA 23111
Phone: +1 (804) 559 6667 • Email: info@impi.org
WWW.IMPI.ORG

Welcome to the 55th IMPI Symposium

Each year, IMPI brings together researchers from across the globe to share the latest findings in microwave and RF heating theories and applications, and this year we have an outstanding array of researchers in attendance. If you are not yet a member of IMPI, we strongly encourage you to join. IMPI membership connects you to microwave and RF academia, researchers, developers and practitioners across the globe.

In light of the ongoing COVID-19 pandemic, this is the second year in our history that IMPI has conducted this Symposium virtually. We would like to thank our technical host: John F. Gerling of Gerling Consulting and our Virtual Exhibitors: Cober, Crescend Technologies, Microwave Techniques LLC, Odyssey Technical Solutions, PSC, SAIREM, Shandong Jaiwei Trading Company, Trumpf Huttinger, QWED and WavePia.

IMPI would also like to recognize the outstanding contributions of Dr. Graham Brodie of the University of Melbourne. For the past five years, Dr. Brodie has lent his expertise to IMPI by serving as the Chairman of the Technical Program Committee. We appreciate his leadership and dedication over the years. IMPI is stronger today because of his service.

Lastly, IMPI would like to express its gratitude to the following individuals:

TECHNICAL PROGRAM COMMITTEE

Chairman
Graham Brodie, University of Melbourne, Australia

Committee Members
Candice Ellison, National Energy Technology Laboratory/LEIDOS, USA
John F. Gerling, Gerling Consulting, USA
John Mastela, EliteRF, USA
Bob Schiffmann, R.F. Schiffmann Associates Inc., USA
Juming Tang, Washington State University, USA

Purchasing Information: Copies of the Proceedings of the 54th Annual Microwave Power Symposium, as well as back issues from prior years, are available for purchase. Contact Molly Poisant, Executive Director of IMPI, at +1 804 559 6667 or molly.poisant@impi.org for details.

Table of Contents

New Technologies

Microwave Chemistry, Food Processing & Industrial Processing II

Poster Presentation

Notes

Notes

Notes

Notes

Creating Materials for High and Ultra-High Temperature Applications using Microwaves and RF

Jon Binner

University of Birmingham, Birmingham, UK

Keywords: Chemical vapour infiltration, microwave, radio frequency, ceramic matrix composites, aerospace

INTRODUCTION

Advanced composites offering a temperature capability significantly exceeding 1200°C, and potentially up to 3000°C, in extreme environments are required for a range of aerospace and other applications [1]. Two types of structural composite are currently being investigated; those based on silicon carbide, SiC (maximum capability ~1500°C) and on ultra-high temperature ceramics (UHTCs), e.g. zirconium diboride, ZrB_2 (max. capability ~2500°C) and hafnium diboride, HfB_2 (max. capability ~3000°C). In each case, the use of fibre reinforcement significantly improves the mechanical performance and, in particular, their toughness and strength. For the SiC-based composites the fibres can be either made of SiC or carbon, C, whilst for the UHTC-based composites the fibres really need to be made of carbon. The composites can be made by a range of different techniques, including:

- *Conventional sintering* – this involves distributing the ceramic powder within the fibre preform (made from a fibre fabric) and then densifying the composite via the process of sintering. The advantage is the simplicity of the process, whilst the disadvantage is that very high temperatures are required that can damage the fibres.
- *Reactive metal infiltration (RMI)* – this involves infiltrating the preform with a molten metal that is then converted to the desired ceramic matrix. The advantage is that it is possible to achieve very high densities, but the disadvantage is that, once again, the very high temperatures involved can damage the fibres.
- *Chemical vapour infiltration (CVI)* – this involves passing a gas through the preform that breaks down at elevated temperature and deposits a solid that forms the matrix. The primary advantage is the low temperature required (typically ~1000°C), the disadvantages are the difficulty in achieving full density and extreme slowness of the process; it can take 3 months to make components. Nevertheless, this process is used commercially, amongst other things, to make carbon /carbon composite aircraft brakes.

This work focuses on the manufacture of both types of composite using CVI, but combines this technology with the use of microwaves (for SiC fibre-based composites) and radio frequency heating (for C fibre-based composites) to speed up the process.

METHODOLOGY

In each case, the composites are composed of three elements, table 1. The ceramic powder is initially impregnated into the fibre preform [2] and then the composites are produced using chemical vapour infiltration, figure 1, with methyltrichlorosilane (MTS) in a hydrogen carrier gas used to create the SiC matrix, equation 1, and methane used to deposit the C matrix, equation 2.

$$CH_3SiCl_{3\,(l)} + H_{2\,(g)} \rightarrow SiC_{(s)} + 3HCl_{(g)} + H_{2\,(g)} \quad [1]$$

$$CH_{4\,(g)} + H_{2\,(g)} \rightarrow C_{(s)} + 3H_{2\,(g)} \quad [2]$$

Table 1. Composite compositional structures

Composite	Fibre (f)	Powder (p)	Matrix (m)
Silicon carbide	SiC	SiC	SiC
UHTC	C	UHTC	C

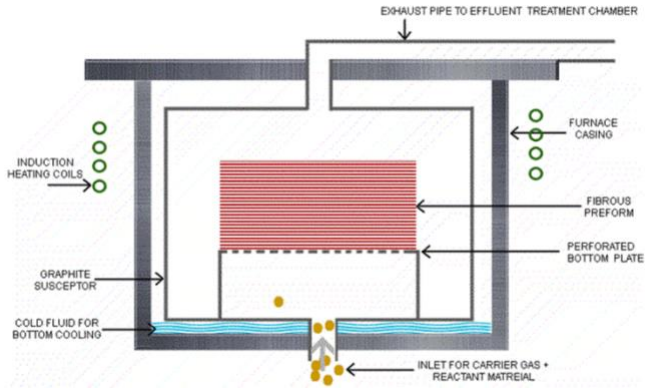

Figure 1. The conventional CVI process.

With conventional, radiant heating, the surface is the hottest part of the component and so is where deposition first occurs. This causes the pore channels that lead through the fibrous preform to become blocked, a process known as crusting. The CVI process then has to be stopped, the part removed, its surface machined and then the whole process started again. This can need doing 3 or 4 times before the part is finished. When combined with a very slow heating rate each time (to minimize the temperature gradients), it is not surprising that the conventional process can take ~1000 hours in total, typically spread over ~3 months.

At the University of Birmingham, in the UK, we have two CVI systems; one uses microwaves (2.45 GHz) and the other radio frequency heating (150-400 kHz). In both cases, the power is absorbed (at least initially) by the fibre preform and the powder that is impregnated into it, though as the matrix is deposited it will also couple. The primary advantage of using electromagnetic heating is that an inverse temperature profile is developed [3], which means that the fibre preform heats from the inside out. Deposition now occurs from the centre of the part, therefore there is no crusting and hence no need to interrupt the process. There is also no need to use extremely slow heating rates to minimize the temperature profile. Thus microwave heating is capable of yielding $SiC_f/SiC_p/SiC_m$ composites in ~100 hours, whilst (for reasons that are still unclear), radio frequency heating

yields $C_f/UHTC_p/C_m$ composites in ~24 hours; factors of approximately x10 and x40 faster respectively.

RESULTS & DISCUSSION

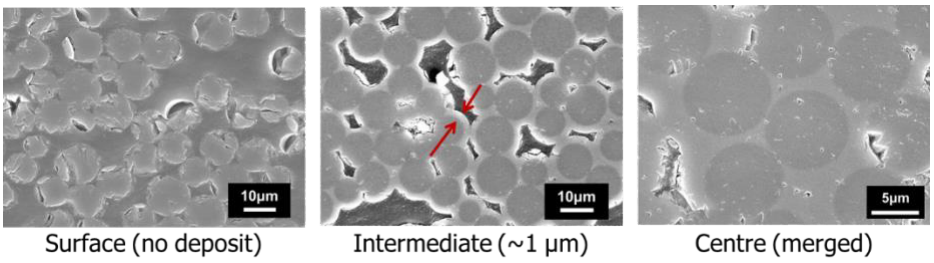

Figure 2. 'Inside out' infiltration of SiC achieved after 4 hours using microwave CVI for a Tyranno ZMI SiC fibre preform made of 20 discs of plain woven fabric stacked & stitched. T = 900°C; P = 200 mbar; MTS/H_2 ratio = 10

Figure 2 illustrates the effect of the inverse temperature profile developed during microwave CVI of $SiC_f/SiC_p/SiC_m$ composites; similar results are obtained for $C_f/UHTC_p/C_m$ composites with RF heating, whilst figure 3 shows a $C_f/UHTC_p/C_m$ composite being tested at ~2300ºC by arc-jet testing. This test is the closest simulation of real-life applications for materials intended for use in rockets and hypervelocity vehicles since it combines extremely high temperatures with gas velocities up to the hypersonic.

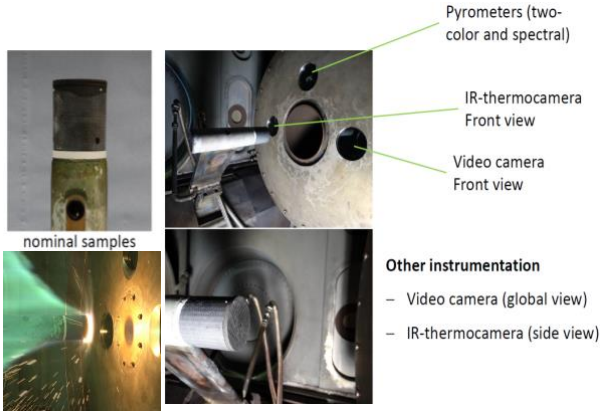

Figure 3. Arc-jet testing of a $C_f/ZrB_{2\ p}/C_m$ composite at ~2300ºC by DLR, Germany.

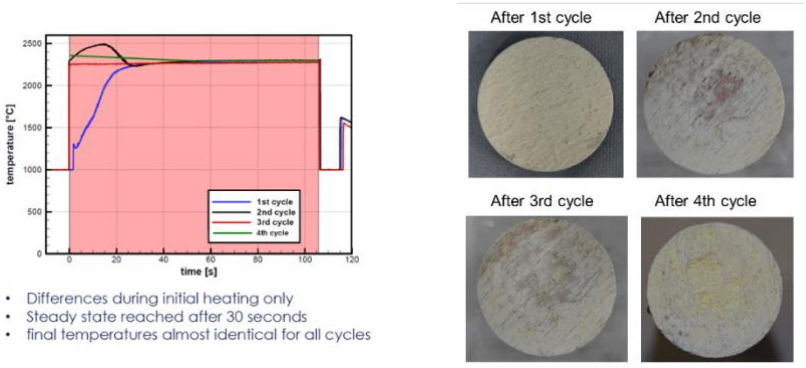

Figure 4. Results from arc-jet testing a $C_f/ZrB_{2\ p}/C_m$ composite at ~2300°C by DLR, Germany.

Figure 4 shows the results of the arcjet tests, both in terms of the heating profile achieved and the resulting appearance of the sample after no less than 4 repeat runs. As can be seen, the sample survived very well indeed and it is believed from the lack of erosion that it could have coped with many more test cycles demonstrating excellent re-usability.

CONCLUSION

The use of electromagnetic heating has permitted ceramic matrix composites to be produced using chemical vapour infiltration in much faster times than with conventional CVI. The benefit arises from the 'inside-out' heating approach that is achieved. The resulting composites display excellent properties and have significant potential for a range of different applications, both in aerospace and other fields.

REFERENCES

[1] Binner J, Porter M, Baker B, Zou J, Venkatachalam V, Rubio Diaz V, D'Angio A, Ramanujam P, Zhang T and Murthy TSRC, 'Selection, Processing, Properties and Applications of Ultra-High Temperature Ceramic Matrix Composites, UHTCMCs – A Review', *International Materials Reviews* **65** [7] 389–444 (2019).

[2] Baker B, Rubio V, Ramanujam P, Binner J, Hussain A, Ackerman T, Brown P, Dautremont I, Development of a slurry injection technique for continuous fibre ultra-high temperature ceramic matrix composites, *J. Eur. Ceram. Soc.* **39** 3927–3937 (2019).

[3] Binner JGP, 'Faster ceramic composites via use of an inverse temperature profile during chemical vapour infiltration', Ceram Trans **83**, Ceramic Processing Science, Eds. Messing GL, Lange FF and Hirano S, Am Ceram Soc, 433-442 (1998).

Preliminary Considerations for Microwave Consolidation/Sintering of Lunar Regolith Simulant

Ralph W. Bruce, Ph.D.[1], Martin Barmatz, Ph.D.[2] , Edwin Ethridge, Ph.D.[1] , Michael R. Effinger[3] , Dan Hoppe, Ph.D.[2], John Huleis[2], William Kaukler, Ph.D.[4] , Tom Meek, Ph.D.[1], Doug Rickman, Ph.D.[4], Javier Sanchez[4] and Holly Shulman, Ph.D. [5]

[1]RWBruce Associates, LLC, Joelton, TN, USA, [2]Jet Propulsion Laboratory, California Institute of Technology, Pasadena, CA, USA, [3]NASA-MSFC, Marshall Space Flight Center, AL, USA [4]Jacobs Space Exploration Group, Huntsville, AL, USA, [5]DrHollyShulman, LLC, Alfred, NY, USA

Keywords: Microwave, Lunar Regolith, Densification, Sintering, Consolidation, HFSS, COMSOL, JSC-1A

INTRODUCTION

As NASA prepares to establish permanent habitats on the Moon, a significant first step is to land multiple times in the same area. As was consistently shown during the Apollo program, the very fine granular structure of the lunar regolith (the Moon's "soil") poses significant physical and health challenges [1]; especially the hyper-velocity lunar surface ejecta that results from the rocket engine exhaust [2]. To mitigate this, the regolith must be consolidated.

A rocket landing pad's thickness should be several inches; therefore, the depth of penetration that microwaves provide has led to its consideration as a primary regolith treatment technology. Lasers and solar heating have also been considered but these technologies lack sufficient penetration depth and lead to reduced pad thickness.

LUNAR REGOLITH – AN UNUSUAL MATERIAL

Heiken, et al [3] suggest that Lunar surface rock is overwhelming composed of minerals that are well known on Earth; however, it is much more complex than any terrestrial rocks. The most obvious differences derive from the lunar history of hypervelocity impacts from large meteorites (>10 km wide), which initially convert the surface to a plasma, a melt or shock crushed rock, to micrometeorites, which create a finely milled rock powder (regolith).

Geologists consider the parent materials of the regolith to be mafic or ultra-mafic igneous rocks, consisting most commonly of silicates: anorthite, various pyroxenes, and olivines. All of these minerals are refractory. Further, essentially everything about the lunar regolith is very unusual compared with terrestrial materials. Chemically, all the constituents in the regolith are extremely reduced, having formed under very low fO2 (fugacity of oxygen), In contrast to terrestrial rocks, there is an absence of H2O and other volatile molecules and radicals like CO, CO2, CO3, SOX, which have formed under vastly higher fO2. The average particle size of the lunar regolith is approximately 50 μm, but because there is no sorting process on the Moon, as there are no fluids present, there is a statistical probability of finding particles of any given size. The regolith also contains metallic iron, glasses of three different origins and varied compositions, intensely shattered minerals, and microscopic vesicles. Some particles are perfect spheres, and some are highly angular. This high angularity minimizes conduction giving rise to a "super insulation" characteristic that is further enhanced because there is no heat convection due to the

moon's vacuum. How these affect the approach to sintering and the implications for the microwave system configuration will be considered.

The lunar regolith is highly heterogeneous, which contrasts radically with commercially processed ceramics and metal oxides that have been treated by microwaves in the past. It is also important to note that the effect of many of the lunar regolith properties on the propagation of microwaves through the regolith is either minimally or very poorly known.

As actual lunar regolith is not readily available, and is not available at all in bulk, simulants must be used for experiments and testing. This of course adds another layer of complication to the work, as the simulants do not and cannot fully replicate all the important characteristics of the actual lunar regolith. For example, the intra-particle textures are beyond our practical reach in making simulants. Also, as the simulants are made from terrestrial feedstocks, they include non-lunar phases that are derived from weathering and/or metamorphic processes. These non-lunar phases are, compared to lunar norms, hyper-oxygenated, and super-hydrated. Their presence in high temperature, microwave processing introduces various non-lunar behaviors in the simulant.

To address all the preceding concerns, basic electrical and materials research by the team is moving along many fronts to help guide and constrain the engineering.

METHODOLOGY

Achieving sufficient energy/power deposition is key to getting densified regolith. We initially simulated regolith heating at 2.45 GHz. Ansys HFSS and COMSOL were used to simulate the interaction of various applicator configurations and the lunar regolith simulant as the simulant is being heated. Ongoing experiments, using material simulants, were also performed at NASA-MSFC to validate the simulated results.

RESULTS AND DISCUSSION

ELECTRICAL PROPERTIES

Well-documented temperature dependent dielectric properties of any material are essential to the design of any microwave-based apparatus that is used in heating. Figure 1, shows dielectric values for JSC1-A, a commonly used simulant that reasonably models the regolith for a possible landing site.

Figure 2 depicts what the dielectric properties look like in terms of an impedance. Note the rapid change in the dielectric properties and the impedance properties at around 1000°C, which is the target sintering temperature. It is this rapid change of properties that is providing one of the challenges for maintaining a sintering versus melting regime. Melting is a physical state of the regolith that is to be avoided.

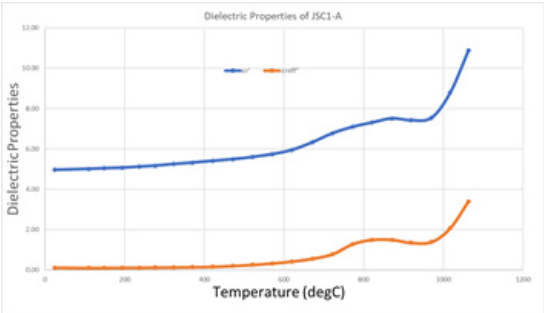

Figure 1: Dielectric properties of JSC1-A over the temperature range of 24°C to 1063°C. [[4], used with permission]

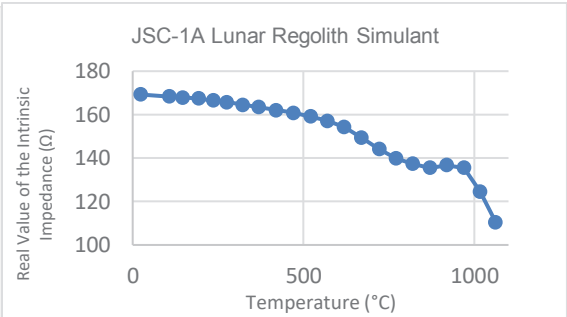

Figure 2: Calculated values of the real part of the intrinsic impedance (from the dielectric values of Figure 1.)

SIMULATION AND EXPERIMENTATION

Part of the effort in applying microwaves is the determination of the best physical structure for irradiating the regolith. Early studies have centered on various open waveguide structures, e.g., straight, down-tapered horn, up-tapered horn, pyramidal horn. Figure 3 shows such a simulation using COMSOL Multiphysics as the simulation engine. Both EM and thermal modules were used to generate the graph. The simulated heating profiles show that, based on the measured dielectric properties of JSC-1A simulant, temperatures at or above 1000°C are achieved in approximately 15 minutes. What is of particular note is that the highest temperatures are just below the surface of the material. Early experiments using a pyramidal horn have resulted in a densified object that was produced just below the surface [Figure 4]. Other simulation tools, e.g. Ansys HFSS, are being used to model other applicator structures.

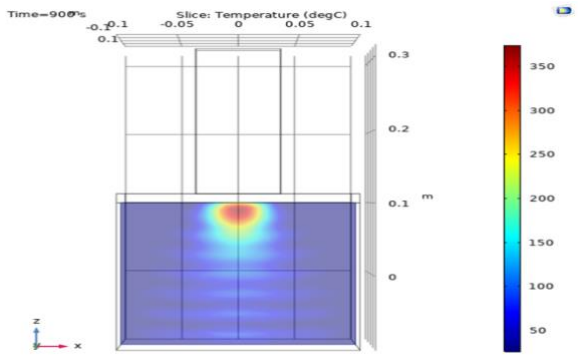

Figure 3: Thermal field assuming bottom of domain is perfectly reflective.

Figure 4: Sintered JSC1-A simulant. Upper surface was approximately 3/8" below the surface.

CONCLUSIONS

Microwave heating to densify/sinter the lunar regolith is being developed. The process of creating the necessary hardware and heating protocols is being developed by a group of engineers and scientist having their expertise rooted in microwave engineering, materials science, geology, physics, electromagnetic and thermal modeling, etc. This team has begun a multi-year effort to be able to get a demonstration device on the moon by 2026.

ACKNOWLEDGEMENT

Some of the research was carried out at the Jet Propulsion Laboratory, California Institute of Technology, under a contract with the National Aeronautics and Space Administration (80NM0018D0004).

REFERENCES

[1] Taylor L, James J**.** Potential toxicity of lunar dust, (2006). *Lunar and Planetary Institute* Website: http://www.lpi.usra.edu/meetings/roundtable2006/pdf/1008.pdf

[2] P.T. Metzger, Dust Transport and Its Effects Due to Landing Spacecraft, , *Lunar Dust 2020*, February 11 -13, 2020, Houston, TX

[3] G.H. Heiken, D.T. Vaniman, and B.M. French (Eds.), *Lunar Sourcebook*, Cambridge University Press, 1991.

[4] Mouris, J. and R. Hutcheon, General Measurement of the Complex Dielectric Constant at the Frequencies 912 MHz and 2466 MHz, *Microwave Properties North*: Deep River, ON.

Performance Validation and Life Expectancy Qualification of a 6kW, 2,450 MHz Magnetron at ~109% of its Maximum Rated Microwave Power

Mohammad Kamarehi[1], Ken Trenholm[1], Francesco Braghiroli[2], Ilya Pokidov[1], Joe Desjardins[1], Francesco Garuti[2]
[1]MKS Instruments / P&RGS, Wilmington, USA
[2]MKS Instruments / Alter Products, Reggio Emilia, Italy

Keywords: Magnetron, Power, Filament Temperature, Efficiency, Spectral Output

INTRODCUTION

Magnetron-based microwave delivery systems of various power levels are widely used in applications such as microwave heating, material processing, research laboratories, as well as Semiconductor remote plasma sources. It is also known that the delivered microwave power downstream from the magnetron module is not the true and specified power generated from the magnetron upstream in the magnetron module and associated delivery system. True delivered power is influenced by the inconsistency of the magnetron efficiency, isolator insertion loss, reflected power as well as other parameters listed in the METHODOLOGY section below. Furthermore, these delivery systems do not compensate for the magnetron efficiency and power degradation as the magnetron ages.

Based on an extensive research performed, in order to deliver a true full rated power to the processing load, a magnetron must potentially operate up to about 109% of its maximum rated power to compensate for power losses incurred in the magnetron module and the delivery system, as well as the continuous drop in the magnetron efficiency, ever so slowly, as the magnetron ages. As such, to compensate and regulate for the power losses upstream from the processing load, a sophisticated power control is also required.

This paper will address a diligent methodology of qualifying a selected 6kW magnetron to continuously operate up to about 109% of its maximum specified power through the magnetron's life expectancy of up to and exceeding 5,000 hours.

METHODOLOGY

Figure 1(a) depicts a Magnetron Delivery System to obtain, evaluate, and validate the operating parameters for a selected 6kW magnetron. A complete set of diagnostic tools and electronic devices are incorporated in order to monitor, control and eventually demonstrating a consistent, viable, and reliable performance at ~109% of the magnetron's maximum rated power. Since the magnetron anode voltage is NEARLY constant and is a

LINEAR function of its magnetic flux, the magnetron current is increased by approximately 9% over its maximum rated value, to the point that ~109% of the rated power is achieved.

The primary operating magnetron parameters and their respective values which are affecting and influencing the true magnetron output power downstream from the delivery components, are listed below as (a) through (g). Some of these operating parameters, such as the optimal filament temperature and moderate anode temperature, are also key to extending the magnetron life vs. a balance magnetron performance.

a) If temperature sensitive magnets such as ceramic type is used, the initial power drop is determined by Po(T)={1-0.0013(T-20}Po, where $T_{initial}$ is assumed to be 20°C.
b) Optimal filament temperature is key to balancing magnetron performance and life.
c) Magnetron efficiency, which varies from magnetron to magnetron.
d) Isolator used to protect the magnetron – so the insertion loss is a source of power loss.
e) Reflected power due to the delivery components as well as the load mismatch.
f) The efficiency degradation as the magnetron ages due to the erosion of anode vane tips.
g) Insufficient anode thermal management for minimizing anode core temperature.

Figure 1(a) is depicting the relevant schematic used to evaluate the magnetron at 109% of its maximum rated power. The evaluation system includes an array of diagnostic components as well as electronic and solid state elements for software control protocol.

Figure 1(b) shows calculated and assumed values for the above parameters listed (a) through (g). Having utilized these parameters, it was found that the magnetron had to operate at ~109% of its maximum rated power to deliver a true 6kW of microwave power downstream to the processing load – and to do so, the magnetron anode current was accordingly increased and regulated continuously at 1,180 mA, ~9% over its maximum rated value.

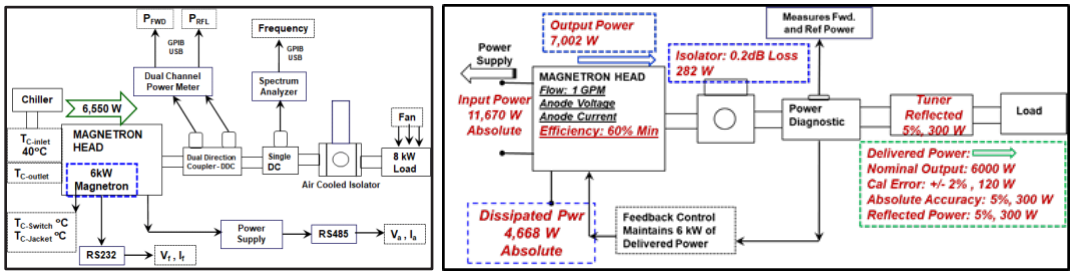

a. High-level Evaluation Schematic b. Parameters Obained to Qualify 109% of Rated Power

Figure 1. High-level Illustration of Qualifying 6kW Magnetron at 109% of its Rated Power

RESULTS AND DISCUSSION

Figure 2. shows the results of the magnetron spectral output for optimizing the magnetron filament temperature to a) avoid over temperature and spectral broad banding b) balance performance and lifetime and c) avoid under temperature and insufficient emission leading to potential moding. How the RESULTs were obtained including the TECHNICAL INTERPRETATION will be described in detail during the IMPI presentation.

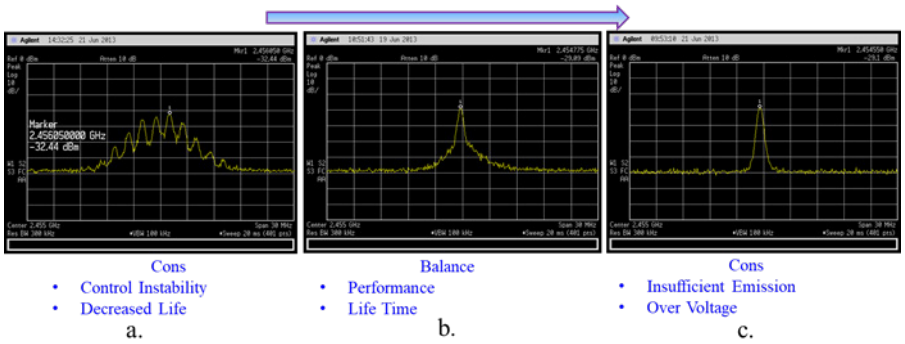

Figure 2. Spectral Output of Maintaining an Optimum Filament Temperature

Figure 3(a) shows the results of the operating parameters of the magnetron of over 5,000 hours with a minimal degradation. The magnetron efficiency dropped only -0.56%. The upstream magnetron output power of ~ 6.55kW obtained and regulated by increasing the anode current to 1,180 mA, ~9% over its maximum recommended value. The magnetron frequency dropped only 1.50 MHz over the life of the magnetron as shown in Figure 3(b).

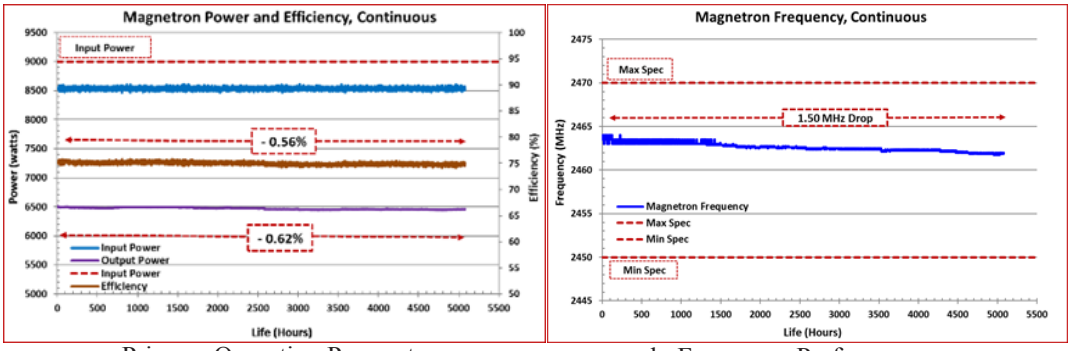

a. Primary Operating Parameters b. Frequency Performance

Figure 3. Results of the Operating Parameters of the Magnetron of over 5,000 hours

CONCLUSION

Extensive research and life test performance has demonstared that a selected 6kW magnetron can be operated at ~%109 of its maximum advertised power to deliver a true 6kW of power downstream to the processing load and the end-user's equipment without any degradation of its operating parameters for the entire typical life of the magnetron.

Kinetic Study of Microwave-assisted Infrared Drying of Germinated Lentils

Tahereh Najib[1] and Venkatesh Meda[1]

[1]University of Saskatchewan, Saskatoon, Canada

Keywords: microwave-assisted infrared drying, thin-layer models, lentils, germination

INTRODUCTION

The increasing demand for a sustainable food system leads food companies to consider germinated pulses as functional ingredients in manufactured food products. However, the enriched germinated pulses need to be dried and milled into flour to facilitate a long-term storable ingredient. The drying process has been widely applied in the food industry. Nevertheless, the need for enhancement of the drying processing, in terms of food quality and energy consumption, still exists. Microwave drying, which produces volumetric heating, has some advantages compared to conventional drying, including improved heat and mass diffusion, shorter processing time, less energy consumption, and quality preservation of biomaterials [1,2]. One of the enhanced microwave technologies is the combination of infrared (IR) radiation with microwave (MW) heating, resulting in reduced drying times, because the moisture transferred to the surface of biomaterial by microwave volumetric heating can be directly and evenly heated by IR radiation [3]. Although there have been many works on microwave drying of different seeds, fruits, and vegetables, no kinetic study exists on microwave-assisted infrared (MW-IR) drying of germinated lentils. Thus, the objectives of this study are introducing a drying system which reduces the process time considerably and providing a model to understand and optimize the drying process.

METHODOLOGY

MW-IR drying of 0-, 1-, 2-, and 3-day germinated lentils (CDC Greenland) was carried out in an oven (Advantium™, General Electric Company, Louisville, USA) with the maximum microwave and infrared power of 700 and 750 W, respectively. The experiments were performed at three levels of microwave and infrared power (20, 60, and 100 % of maximum microwave power and 0, 50, and 100 % of maximum infrared power) until the seeds reached a moisture content of below 10 %.

The experimental data were fitted by using four different thin-layer drying models namely Newton, Page, logarithmic, and diffusion approach models. The models are expressed based on MR and time (min). The best model to predict the behaviour of MW-IR drying was chosen based on two statistical parameters, including the coefficient of determination (R^2) and root mean square error (RMSE) [3,4]. To compare the effect of

MW and IR power on water diffusion in a thin-layer of germinated lentils, surface diffusion coefficient (D_{eff}) was calculated based on Fick's second law from the slope of $\ln M_R$ versus time (s) for drying of 1-day germinated lentils using different powers of MW and IR [4].

RESULTS

The results of modeling with thin-layer drying models are presented in Table 1. The coefficient of determination (R^2) and root mean square error (RMSE) of the models varied from 0.752 to 0.996, 0.900 and to 0.022, respectively. The Fick's second law shows that the surface diffusion coefficient increased in the range of 1.51×10^{-9} to 1.79×10^{-8} m^2/s with increasing MW and IR power (Fig 1).

Table 1. Statistical coefficients to investigate the performance of drying of germinated lentils

Kinetic models		MW (%): 20			MW (%): 60			MW (%): 100		
		IR (%)			IR (%)			IR (%)		
		0	50	100	0	50	100	0	50	100
Newton	k	0.037	0.106	0.142	0.134	0.205	0.227	0.169	0.224	0.258
	R^2	0.991	0.941	0.926	0.978	0.953	0.922	0.946	0.926	0.752
	RMSE	0.031	0.082	0.095	0.052	0.073	0.098	0.081	0.095	0.900
Page	k	0.0302	0.030	0.033	0.036	0.078	0.105	0.083	0.072	0.086
	n	1.063	1.063	1.544	1.738	1.273	1.454	1.728	1.512	1.701
	R^2	0.993	0.987	0.996	0.993	0.991	0.991	0.988	0.995	0.994
	RMSE	0.029	0.039	0.022	0.029	0.032	0.033	0.038	0.026	0.028
Logarithmic	a	1.048	1.930	4.335	1.145	1.526	2.354	1.381	2.085	3.379
	k	0.034	0.044	0.023	0.122	0.120	0.077	0.119	0.091	0.060
	c	-0.042	-0.893	-3.295	-0.088	-0.475	-1.295	-0.311	-1.017	-2.308
	R^2	0.993	0.984	0.996	0.990	0.989	0.984	0.981	0.988	0.982
	RMSE	0.029	0.044	0.024	0.035	0.036	0.044	0.050	0.039	0.048
Diffusion approach	a	-1.930	-21.680	44.360	13.960	34.100	-48.940	9.788	230.200	17.610
	b	0.857	0.958	0.943	0.946	0.936	0.978	1.113	0.997	0.772
	k	0.057	0.239	0.031	0.068	0.049	0.543	0.361	0.126	0.039
	R^2	0.993	0.985	0.982	0.986	0.985	0.987	0.988	0.947	0.968
	RMSE	0.029	0.043	0.047	0.041	0.042	0.040	0.038	0.082	0.065

DISCUSSION

The Page model, with the highest value of R^2 and the lowest values of root mean square error shows the best performance in describing the thin-layer MW-IR drying process of germinated lentils. The Fick's second law stated that by increasing the MW and IR power, the drying efficiency increases, however the balance between microwave power and infrared power is a determining factor in diffusion ability. For example, although the

microwave power is higher in 100-0% of maximum MW-IR power compared to 60-50%, the surface diffusion coefficient is higher in the second case. The 60% of maximum MW power can evaporate the inside moisture, transfer it to the surface, and make it ready for IR radiation. In the 20-100% of maximum MW-IR power, although the IR power is twice that of the previous treatment, the 20% of maximum MW power is too small to evaporate enough water from the inside for the IR heating.

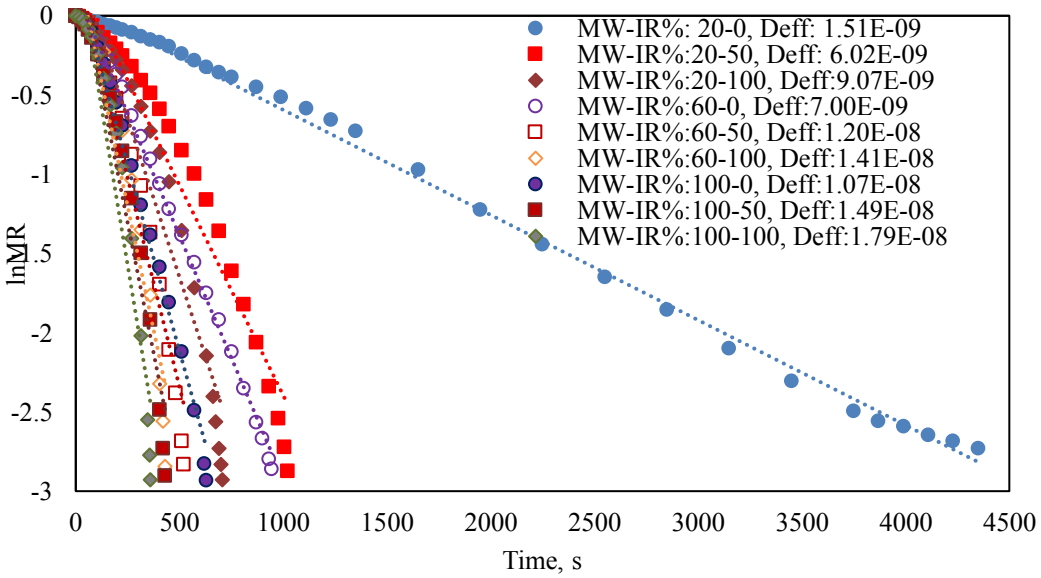

Figure 1. Linear fitting curve of Fick's second law for different MW-IR powers

CONCLUSION

The microwave assisted-infrared drying process, which reduces drying time significantly, can be modelled and explained well by thin-layer kinetics models. Moreover, the Fick's second law of diffusion can be applied to describe the moisture diffusion in germinated lentils.

REFERENCES

[1] Q. Guo, D.W. Sun, J.H. Cheng, and Z. Han, Microwave processing techniques and their recent applications in the food industry, *Trends Food Sci. Technol.*, vol. 67, pp. 236-247, 2017.

[2] M. Shaw, V. Meda, L. Tabil Jr., and A. Opoku Jr., Drying and color characteristics of coriander foliage using convective thin-layer and microwave drying, *JMPEE*, vol. 41, pp. 56-65, 2006.

[3] M.M. Heydari,B.S. Kauldhar, and V. Meda, Kinetics of a thin-layer microwave-assisted infrared drying of lentil seeds, *Legum. Sci.*, vol. 2, no. 2, pp. e31, 2020.

[4] J. Du, L. Gao, Y. Yang, S. Guo, J. Chen, M. Omran, and G. Chen, Modeling and kinetics study of microwave heat drying of low grade manganese ore, *Adv Powder Technol*, vol. 31, no. 7, pp. 2901-2911, 2020.

Microwave Assisted Curing Process for Thermosetting Polymers

Carlos J. Cancio[1], Stephan Holtrup[2]and Klaus Werner[2]

[1]Bodus GmbH, Aarau, Switzerland
[2]pinkRF, Nijmegen, Netherland

Keywords: microwave assisted curing, epoxy resin, thermosetting polymers, microwave assisted process, dielectric heating, dielectric properties.

ABSTRACT

Techniques using microwaves as a volumetric heating source are used in a variety of applications and technical disciplines. One of this applications is the microwave-assisted curing of epoxy resins or fibre-reinforced composites.

Using mechanical testing carried out on conventional oven cured and microwave cured specimens, it was found that microwave-assisted localised heating is a promising technique to significantly improve the mechanical properties of polymer reinforced sandstone for wellbore reinforcements, i.e. the microwave cured specimens showed higher yield stress, compressive strength and toughness compared to conventional cured specimens. [1]

Processing times and curing temperatures are important issues in many applications where thermosetting polymers are used. Particularly, heat energy must be used in order to initiate curing of the polymer at somewhat elevated temperatures, approximately 80°C. At the same time, good quality cured polymers, for example in terms of mechanical properties and glass transition temperatures must be achieved. Therefore, methods and techniques which allow for fast and efficient heating and still leading to the expected material properties are required.

Solid state RF generators were used to irradiate polymer matrix based composite samples with microwave power at 2.45 GHz. These sources allowed a precise control and reproducibility of the amount of energy delivered to the relatively small samples. The samples were placed in a WR 430 waveguide with an in-situ monitoring of the samples' surface temperature. A reduction in curing time compared to conventional methods was clearly observed. Additionally, a microstrip test setup was used to determine the dielectric properties of the epoxy composite during the curing process.

Details on the experimental setups and methods used as well as measured results will be presented.

REFERENCES

[1] Chinedum Ogonna Mgbemena et al., Accelerated microwave curing of fibre-reinforced thermoset polymer composites for structural applications: A review of scientific challenges, *Composites Part A: Applied Science and Manufacturing, Volume 115, 2018,* pp. 88-103, https://doi.org/10.1016/j.compositesa.2018.09.012

Microwave Treatment Effect on Faba Bean and Wheat Grains' Nutritive Value as Animal Concentrate Feed

M. S. R. Shishir[1, 3, *], G. Brodie[2], B. Cullen[2], and L. Cheng[1]

[1]The University of Melbourne, Melbourne, Dookie Campus, VIC 3647, Australia.
[2]The University of Melbourne, Parkville, VIC 3010, Australia.
[3]Department of Animal Nutrition, Bangladesh Agricultural University, MYM 2202, Bangladesh

Keywords: grains; microwave treatment; digestibility; moisture; animal concentrate feed.

INTRODUCTION

Grain is the vital component of supplement concentrate feed for ruminant animals. It ensures ruminant production and improves nutritive value, which provides more productivity even with limited supplementation. However, due to high prices and high demand for human and other monogastric animals' consumption, grain availability in the ruminant diet is often limited. Microwave (MW) heating is one of the most efficient and established processing methods in the food industry and other industries [1]. Quick time processing and efficient energy consumption make MW heat technology more suitable for different purposes. Some studies have shown that MW heating might have the potential to improve forage hay and grain nutritive value [2-4]. However, thus far no studies were conducted to determine MW heat treatment's effect on faba bean *(Vicia faba);* while limited studies on wheat (*Triticum aestivum)* treated with MW treatment were found. The previous study also added moisture before MW treatment, and no data was found on grain treated with MW without adding moisture. Therefore, this study aims to observe MW heat treatment's effect on faba bean and wheat grain *in vitro* digestibility, and other nutrient content, without adding moisture.

METHODOLOGY

The study was conducted at The University of Melbourne Dookie Campus, Australia.

The experimental design was comprised of five MW treatments, applied to two grains, which are commonly used for sheep production in northern Victoria, Australia. Each grain × MW treatment had three replications. Each replication of 50 gm was subjected to MW treatment.

Two types of grain faba bean (*Vicia faba*) and wheat (*Triticum aestivum*) grain were collected from the Dookie campus farm, the University of Melbourne VIC, Australia.

According to the designed MW treatment, Grain samples were subjected to five MW treatment times **(0, 15, 30, 45, and 60 seconds)**, using a bench-scale MW oven (EMS8586V, Sanyo, Tokyo, Japan). The MW oven had a cavity dimension of 370 mm × 380 mm × 210 mm, an operational frequency of 2.45 GHz, and a rated power level of 1.4

kW (Actual average MW power provided approximately 700w (50%) according to equation from [5]). Based on the pre-experimental test, the maximum MW treatment time (60 s) in this study was selected as it was the closest time to the grain browning point.

According to the Association of Official Analytical Chemistry, all the samples were analyzed for proximate components [6]. The acid detergent fiber (ADF) % and neutral detergent fiber (NDF) % of the forage samples were determined by boiling the samples, while sealed in nylon bags, in an ANKOM 220 Fiber Analyzer (F57 filter bag, ANKOM Technology, Fairport, USA) using acid detergent and neutral detergent solutions, respectively [7]. The *in vitro* pepsin-cellulase digestibility was determined as described by the Australian Fodder Industry Association Manual [8], from the Department of Primary Industries, Victoria, Australia.

The recorded data were analyzed using one-way analysis of variance (ANOVA) by the statistical software Genstat 16th Edition. The least significant difference (Fisher's protected) among treatments and microwave treatment times was calculated to distinguish among means at a 95% confidence level.

RESULTS

The dry matter content increased with increasing MW treatment time. A significant difference was observed in wheat ADF and NDF content (Table 1). Both Faba bean and wheat CP content increased significantly at MW treatment time 45 and 15 seconds, respectively. In dry matter digestibility (DMD), Faba bean showed the highest increase of DMD at 30 seconds, whereas wheat showed a slight increase of digestibility at 15 seconds MW treatment time compared to control (Table 1).

Table 1: Effect of microwave treatment on Faba bean and wheat grain nutritive value

Grain	MW Treatment	DM (%)	ADF (%)	NDF (%)	CP (%)	DMD (%)
Bean	0 s	91.7^{d}±0.2	12.6±1.6	24.7±1.5	23.5^{bc}±0.7	86.6^{b}±0.8
	15 s	91.7^{d}±0.0	16.0±0.3	24.4±2.0	23.1^{c}±1.3	91.0^{a}±1.0
	30 s	92.7^{c}±0.3	16.6±1.6	24.5±0.3	24.3^{abc}±1.1	93.0^{a}±1.5
	45 s	94.5^{b}±0.1	16.9±0.5	25.8±1.3	25.1^{ab}±0.3	87.5^{b}±0.2
	60 s	97.0^{a}±0.1	17.7±1.8	26.9±0.9	25.9^{a}±0.4	87.1^{b}±1.0
SED		0.16	2.11	1.09	0.69	0.82
P value		<0.001	0.155	0.182	0.014	<0.001
Wheat	0 s	89.8^{d}±0.1	11.0^{c}±0.7	18.9^{d}±0.7	13.3^{bc}±0.4	96.8^{ab}±0.3
	15 s	90.2^{d}±0.2	12.3^{bc}±0.8	20.7^{c}±1.5	15.0^{a}±0.5	97.3^{a}±0.4
	30 s	91.5^{c}±0.3	14.4^{ab}±0.6	22.1^{bc}±0.5	12.7^{c}±0.1	96.2^{b}±0.5
	45 s	93.8^{b}±0.4	14.9^{a}±0.8	23.4^{ab}±0.9	14.0^{ab}±1.2	96.0^{b}±0.3
	60 s	95.6^{a}±0.2	14.6^{a}±2.4	24.1^{a}±0.4	13.1^{bc}±0.6	96.1^{b}±0.6
SED		0.21	1.04	0.73	0.54	0.36
P value		<0.001	0.014	<0.001	0.013	0.021

DISCUSSION

With the increasing MW treatment time, each grain's dry matter content (DM) was increased significantly, which is attributed to the rapid diffusion of intercellular moisture due to MW heating [9]. The dry matter digestibility (DMD) of faba bean increased by 7.4% when treated for 30 seconds (<0.001) in comparison to control, whereas wheat showed an increase of 0.5% when treated for 15 seconds ($P = 0.021$). The DMD changes may be due to cell wall rupture, which happened due to high-pressure steam explosion as a result of MW heating [10]. A significant increase was observed in the crude protein (CP) content of faba bean and wheat grain. A 10 and 13% increase of crude protein was observed in faba

bean (P = 0.014) and wheat (P = 0.013) when treated with MW for 60 and 15 seconds, respectively, by comparison to the control. However, the changes were not observed in the previous study. Acid detergent fiber (ADF) content increased by 36% in wheat grain when treated for 45 seconds, whereas Neutral detergent fiber (NDF) content increased by 27% in wheat grain when treated for 60 seconds, in comparison to the control. No significant difference was observed in Faba bean ADF or NDF content, which also supports the increase in faba bean DMD content. However, further study is required to understand the mechanism for changing the nutritive value of faba bean and wheat grain.

CONCLUSION

The current study suggests that MW treatment can improve the nutritive value of faba bean and wheat grain. However, overheating with MW treatment can increase ADF and NDF.

REFERENCES

1. Ayappa, K., et al., *Microwave heating: an evaluation of power formulations.* Chemical engineering science, 1991. **46**(4): p. 1005-1016.
2. Brodie, G., et al., *The Effect of Microwave Treatment on Animal Fodder.* Journal of Microwave Power and Electromagnetic Energy, 2012. **46**(2): p. 57-67.
3. Ebrahimi, S., A. Nikkhah, and A. Sadeghi, *Changes in nutritive value and digestion kinetics of canola seed due to microwave irradiation.* Asian-Australasian Journal of Animal Sciences, 2010. **23**(3): p. 347-354.
4. Sadeghi, A. and P. Shawrang, *Effects of microwave irradiation on ruminal protein degradation and intestinal digestibility of cottonseed meal.* Livestock science, 2007. **106**(2-3): p. 176-181.
5. Brodie, G., S. Hamilton, and J. Woodworth, *An assessment of microwave soil pasteurization for killing seeds and weeds.* Plant Protection Quarterly, 2007. **22**(4): p. 143.
6. Helrich, K., *Official Methods of analysis of the Association of Official Analytical Chemisty.* 1990.
7. Van Soest, P.J., J. Robertson, and B. Lewis, *Methods for dietary fiber, neutral detergent fiber, and nonstarch polysaccharides in relation to animal nutrition.* Journal of dairy science, 1991. **74**(10): p. 3583-3597.
8. AFIA, *Laboratory methods manual: a reference manual of standard methods for the analysis of fodder*. 2011, Australian Fodder Industry Association Ltd Melbourne.
9. Brodie, G., *Simultaneous heat and moisture diffusion during microwave heating of moist wood.* Applied Engineering in Agriculture, 2007. **23**(2): p. 179-187.
10. Shishir, M.S.R., et al., *Microwave Heat Treatment Induced Changes in Forage Hay Digestibility and Cell Microstructure.* Journal of Applied Sciences, 2020. **10**(22): p. 8017.

Microwave Soil Disinfestation for Strawberry Production

Graham Ian Brodie[1], Muhammad Jamal Khan[1], and Scott Mattner[2]

[1] School of Agriculture and Food, The University of Melbourne, VIC, Australia.
[2] Victorian Strawberry Industry Certification Authority, VIC, Australia.

Keywords: Microwave, Disinfestation, Pathogen Control

INTRODUCTION

Chemical fumigants, such as methyl bromide, have traditionally been used for biosecurity and soil disinfestation in agricultural systems. A benefit of chemical soil disinfestation is significant crop yield increases, compared with non-treated soil. Concerns over environmental and health impacts, along with international agreements, are removing these chemicals from circulation. Methyl bromide, in particular, has been banned for non-quarantine uses [1] because it depletes the ozone layer and is harmful to beneficial organisms, operators and the public. Alternative fumigation systems must be found. Soil steaming has been under consideration for some time, especially in Europe [2-5]. Microwave soil heating has also been considered as a viable soil disinfestation tool. This paper reports on a preliminary comparison of microwave soil heating with soil steaming and fumigation with methyl bromide for strawberry production.

METHODOLOGY

Two volumes of topsoil were taken from an experimental section of a commercial strawberry runner producing farm at Toolangi, Victoria, Australia (37° 32' S, 145° 28' E). One of the soil volumes was taken from a section of the site, which had its soil fumigated with methyl bromide (methyl bromide/chloropicrin 50:50, 500 kg/ha) by a commercial contractor (R&R Fumigation Services) under special dispensation from the United Nations. The other volume of soil was taken from a section of the site, which had not been fumigated for three years and could be regarded as untreated.

A 140 kg portion of the unfumigated soil was steam treated in a system, with a nameplate electrical rating of 28.8 kW, for 90 minutes, until the soil reached a uniform 90 °C. Therefore, this steam treatment required 1.1 MJ kg^{-1} of soil. All the soils (fumigated, steamed, and untreated) were then placed into forty 10 cm pots (Figure1). Ten of the untreated pots were heated in a microwave oven (rated at 900 W of microwave power) with a nameplate electrical power rating of 2.25 kW. Each pot of soil weighed 2.9 kg and each pot required 150 s of heating to achieve 90 °C, based on earlier crop responses to microwave soil heating [6]. Therefore, this microwave treatment required 0.12 MJ kg^{-1} of soil. The final experiment consisted of four treatments (untreated control, methyl bromide fumigated soil, steam treated soil and microwave treated soil) with 10 replications. Each

pot had a single strawberry plant transplanted into it (cv. Albion) and the pots were placed in growth cabinets, which were programmed to provide good conditions for strawberry growth (Temperature: 20 °C to 29 °C; 14-hour photo period). Pots were maintained at field capacity moisture content throughout the experiment.

Plants were monitored for stolon growth (vegetative reproductive structures), daughter plants, fruit number and fruit fresh weight over a period of 3 months. Data was analyzed using a single factor Analysis of Variance.

Figure 1 Subset of experimental pots used in the experiment. This image was captured early in the experiment. From left to right: 2 controls, 2 steamed, 2 fumigated and 3 microwave treated pots.

RESULTS

Despite providing good growth, there was considerable variability between plants within each treatment. In most production parameters, microwave soil treatment was significantly better than steam treatment and the untreated control (Table 1). In most parameters, microwave treatment was statistically similar to the fumigated treatment (Table 1). Several of the control pots also grew weeds and fungus was noted on the fruits; however, very few weeds and no fungus were evident in the other soil treatments (Figure 2).

Table 1: Strawberry reproductive and production performance according to individual treatments.

Treatment	Parameter					
	No. of Stolons	Length of Stolons (cm)	Stolon Fresh Weight (g)	No. of Daughter Plants	No. of Fruit	Fresh Weight per pot (g)
Control	1.2^{a}	48.0	7.5^{ab}	1.2^{a}	2.5^{a}	14.9^{b}
Steamed	0.7^{a}	36.1	4.0^{a}	0.9^{a}	1.6^{a}	5.8^{a}
Fumigated	2.2^{b}	82.4	17.6^{c}	3.0^{b}	2.6^{a}	14.6^{b}
Microwaved	2.1^{b}	43.8	10.2^{b}	2.3^{b}	5.0^{b}	21.5^{b}
LSD (P = 0.05):	0.7	35.0	5.2	1.0	1.6	7.4

Note: means with different superscripts in each of the columns are statistically different from one another

DISCUSSION

Although fumigation provided the best results across the measured parameters, microwave soil treatment was statistically similar to soil fumigation in many parameters.

Soil steaming has been proposed as a viable alternative for soil fumigation; however, in this experiment it was consistently the poorest performer across most of the measured parameters. In comparison to microwave soil heating, steam treatment also required significantly more energy to achieve the target temperature of 90 °C. Similar results from microwave soil heating have been found before [6].

Figure 2 Subset of experimental pots illustrating differences between treatments, approximately 6 weeks after crop transplant. Note: the tall plant in the control pot on the left is a weed (*Amaranthus retroflexus*).

CONCLUSION

Microwave soil treatment has potential as a soil fumigation strategy in the strawberry industry. It provides similar performance to current soil fumigants and performed better than steam treatment, which is already being promoted as an alternative fumigation strategy.

REFERENCES

[1] C. A. Carter, J. A. Chalfant, R. E. Goodhue, F. M. Han and M. DeSantis, The Methyl Bromide Ban: Economic Impacts on the California Strawberry Industry, *Review of Agricultural Economics,* vol. 27, no 2, pp. 181-197, Summer 2005.

[2] C. M. Rainbolt, J. B. Samtani, S. A. Fennimore, C. A. Gilbert, K. V. Subbarao, J. S. Gerik, A. Shrestha and B. D. Hanson, Steam as a Preplant Soil Disinfestant Tool in California Cut-flower Production, *HortTechnology,* vol. 23, no 2, pp. 207-214, April 1, 2013 2013.

[3] J. B. Samtani, C. Gilbert, J. Ben Weber, K. V. Subbarao, R. E. Goodhue and S. A. Fennimore, Effect of Steam and Solarization Treatments on Pest Control, Strawberry Yield, and Economic Returns Relative to Methyl Bromide Fumigation, *HortScience,* vol. 47, no 1, pp. 64-70, January 1, 2012 2012.

[4] P. Gay, P. Piccarolo, D. Ricauda Aimonino and C. Tortia, A high efficiency steam soil disinfestation system, part I: Physical background and steam supply optimisation, *Biosystems Engineering,* vol. 107, no 2, pp. 74-85, 10// 2010.

[5] P. Gay, P. Piccarolo, D. Ricauda Aimonino and C. Tortia, A high efficacy steam soil disinfestation system, part II: Design and testing, *Biosystems Engineering,* vol. 107, no 3, pp. 194-201, 11// 2010.

[6] G. Brodie, M. J. Khan and D. Gupta, Microwave Soil Treatment and Plant Growth, In *Sustainable Crop Production* IntechOpen, 2019.

Microwave Atmospheric Plasma Processed Air and Argon for Disinfection of Lentil from BGM

Saeedeh Taheri[1], Graham Ian Brodie[1], Dorin Gupta[1,] and Mohan V. Jacob[2]

[1] School of Agriculture and Food, The University of Melbourne, VIC, Australia.
[2] College of Science and Engineering, James Cook University, QLD, Australia.

Keywords: Microwave, Plasma, lentil, disinfection, BGM

INTRODUCTION

Seed borne fungal pathogens of grains are serious threats to crop yields due to a lack of resistant crop varieties. The use of fungicides to combat these pathogens raises concerns, due to their environmental and health impacts. Therefore, there is a growing demand for the development of more sustainable and environmentally friendly technologies for crop protection. Botrytis Grey Mold (BGM), which is seed-borne, is one of the serious pathogens of a lentil crop and is primarily controlled by chemical fungicides [1]. Processed air from a microwave plasma has previously shown an antimicrobial effect on fresh produce [2]. Therefore, the present study aimed to explore the potential of a microwave plasma processed air for disinfection of lentil seeds from BGM.

METHODOLOGY

The microwave plasma system is illustrated in figure 1. Lentil seeds were artificially inoculated with BGM spores before placing 2.5g of infected seeds in 500-ml glass bottles for treatment. Samples were located, as a single layer, at the bottom of the bottle. The plasma was created with a gas flow of 20 nl min^{-1} of air or a combination of air and argon at a microwave power of 800 W. A 25-cm distance from the end of the quartz tube to the neck of the bottle, which itself had a 177 mm distance from the plasma source, was maintained during the treatment. The seeds were exposed to the plasma for different treatment times, followed by tightly capping the bottles and holding them for different durations (holding time) before performing both quality and microbiological analyses on the seeds. The presence of BGM on the seeds was evaluated by subculturing them on Botrytis Selective Media (BSM). Germination and antioxidant enzyme activities were measured, as indicators of seed quality, based on the procedure explained elsewhere [3].

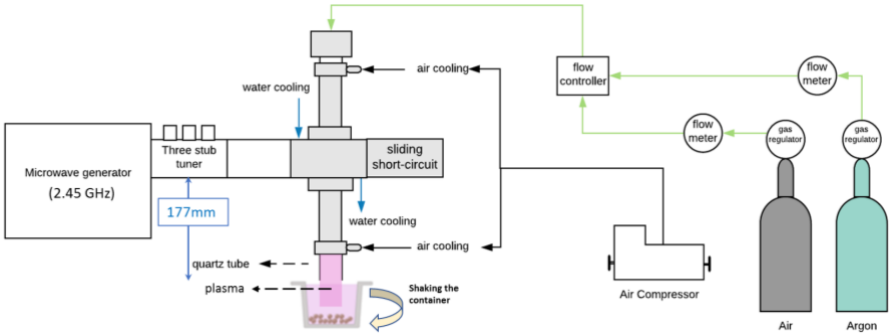

Figure 1 Schematic diagram of the microwave plasma apparatus used in the experiment.

RESULTS

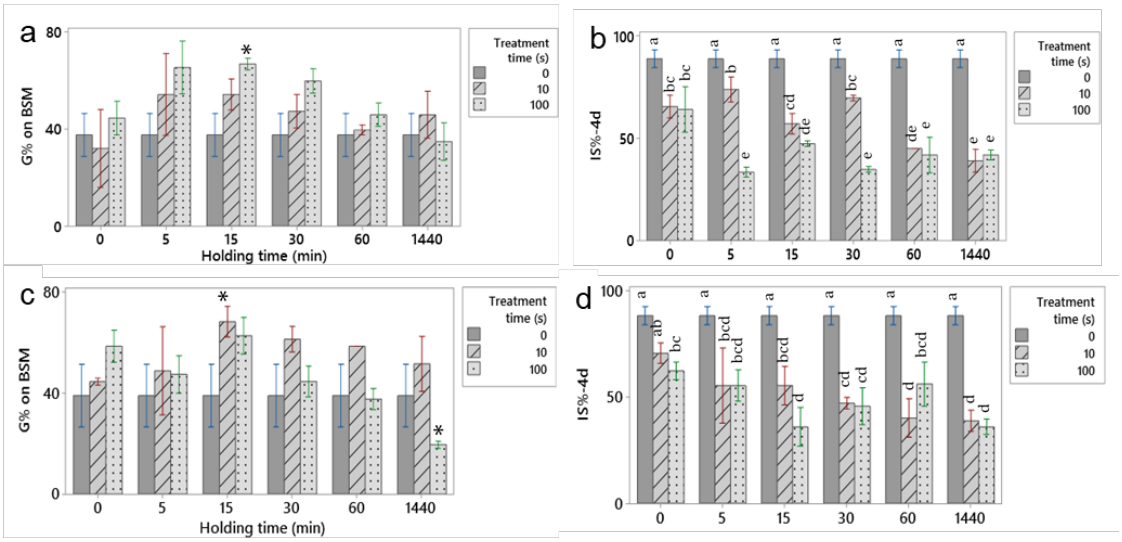

Figure 2 a and c: Germination% (G%) of the contaminated seeds on BSM, b and d: Infected seeds% after 4 d of incubation (IS%-4d), for lentil seeds exposed to 100% air plasma remotely (a and b) and to 30% air/70% argon plasma (c and d) at different treatment.

Table 1 Antioxidant enzymes activities of lentil seedlings before and after the treatments with direct and remote plasma, CAT: catalase, POX: peroxidase, SOD: superoxide dismutase *

Air /Argon%	Treatment time (s)	Holding time	CAT (mM H2O2 mg^{-1} min^{-1})		POX (mM guaiacol mg^{-1} min^{-1})		SOD (Unit mg^{-1})		H_2O_2 (μmole g^{-1})	
100/0	100	5 min	1.02 ±0.10	ab	7.88 ±0.62	a	57.82 ±3.26	a	0.78 ±0.02	ab
	10	24 h	0.99 ±0.06	abc	8.09 ±0.56	a	58.32 ±3.72	a	0.67±0.07	bc
30/70	100	15 min	0.94 ±0.07	abc	8.96 ±0.69	a	54.50 ±10.4	a	0.90 ±0.02	a
	10	24 h	1.10 ±0.06	a	7.876±0.76	a	51.15 ±2.10	a	0.63 ±0.02	c
0/0	Control	-	0.81 ±0.04	bc	8.46 ±0.49	a	56.69 ±7.01	a	0.88 ±0.04	a

* data are ±SE with n=6; numbers in each column that do not share a letter are significantly different according to Fisher's LSD method with 95% confidence level.

DISCUSSION

Treatment of the seeds with 100% air plasma for 100 s and using a holding time of 5 min reduced the seeds' infected rates from 88% to 33% (figure 2, b). Approximately the same reduction in the infected seeds could be achieved by 10 s treatment and 60 min holding time (44%). These treatments did not affect seeds germination while the 100 s treatment, followed by 15 min holding time, significantly increased their germination from 38% to 70% (figure 2, a). This treatment also reduced the infected seeds by about 50%. Applying the 30% air and 70% argon plasma reduced the infected seeds after 10 s of treatment at any holding times from 5 min to 24 h. However, the reduction of infected seeds was not significantly affected by increasing the treatment time from 10 s to 100 s. A 10 s treatment followed by a 15 min holding time reduced the seeds' infection rate from 88% to 58% and significantly increased germination from 38% to 68%. By comparing the results of the two plasmas, it can be observed that the catalase activity of the seeds, which were treated with 30% air plasma, increased after 10 s treatment and 24 h holding time. The water droplet contact angle for these seeds decreased (data not shown), which could be the result of lipid peroxidation of the seed surface, because of the exposure to the reactive species of the plasma.

Any reduction in the infected seeds during the treatment of the seeds with the afterglow of plasma could be the results of bombardment with the reactive species from argon and air. However, the pathogen elimination during the holding times could stem from the exposure to the long-lived species (such as singlet oxygen) as well as the species resulting from their reactions. Here, the damage to the pathogen might be due to exposure to singlet oxygen which led to structural or permanent damage to the spores due to oxidation. The other explanation of pathogen damage during the holding time could be penetration of atomic oxygen and nitrogen into the stack of surface spores, molecular collisions and production of UV radiation, and finally damage of the pathogen [4].

CONCLUSION

Treatment of lentil seeds by a combination of the afterglow of atmospheric microwave plasma and holding them in the trapped processed gas could significantly reduce the BGM infected seeds and consequently increase their germination.

REFERENCES

1. Lindbeck, K., T. Bretag, and R. Ford, *Survival of Botrytis spp. on infected lentil and chickpea trash in Australia.* Australasian Plant Pathology, 2009. **38**(4): p. 399-407.
2. Schnabel, U., et al., *Decontamination and sensory properties of microbiologically contaminated fresh fruits and vegetables by microwave plasma processed air (PPA).* Journal of food processing and preservation, 2015. **39**(6): p. 653-662.
3. Taheri, S., G. Brodie, and D. Gupta, *Fluidisation of lentil seeds during microwave drying and disinfection could prevent detrimental impacts on their chemical and biochemical characteristics*. LWT, 2020. **129**: p. 109534.
4. Moisan, M., et al., *Sterilization/disinfection using reduced-pressure plasmas: some differences between direct exposure of bacterial spores to a discharge and their exposure to a flowing afterglow.* Journal of Physics D: Applied Physics, 2014. **47**(28): p. 285404.

Prediction of Material Dielectric Permittivity by Machine Learning

Candice Ellison[12], Robert Tempke[1,3], Shivani Panyda[4], and Dushyant Shekhawat[1]

[1]National Energy Technology Laboratory, Morgantown, WV, United States
[2]Leidos Research Support Team, Morgantown, WV, United States
[3]West Virginia University, Morgantown, WV, United States
[4]Louisiana State University, Baton Rouge, LA, United States

Keywords: Dielectric permittivity, prediction, machine learning, convolutional neural network.

INTRODUCTION

At microwave frequencies, knowledge of material dielectric permittivity can help predict the attenuation of electromagnetic energy within a material and the loss mechanism by which it generates heat. These characteristics are critical in microwave engineering to optimize microwave system design for a particular process or application. A material's dielectric response is complexly dependent on its chemical and physical properties and is measured by specialized equipment (network analyzer, cables, and test fixture). When dielectric measurement equipment is not available, it would be useful to be able to estimate permittivity from routinely measured or commonly reported material properties. Due to the complexity of material permittivity-property relationships, dielectric permittivity cannot be predicted by a single material property, nor can it be modeled by simple regression equations. By use of machine learning, it is possible to deconvolute these complex relations to predict dielectric permittivity of materials by knowledge of routinely measured material properties, making permittivity estimation possible when expensive dielectric measurement equipment/facilities are not easily accessible or available. In the present work, a neural network is developed to predict static dielectric permittivity based on input material properties (crystal structure, density, and chemical formula). This prediction network serves as a baseline for future work that will extend its capability to frequency-dependent permittivity predictions.

METHODOLOGY

A convolutional neural network (CNN) was developed to predict static dielectric permittivity of materials. An open source material property database (Materials Project) was used to source the input training data for a CNN. In total, data from 3379 oxide materials were used as input data to train the neurlal network and the selected prediction parameters were crystal structure (extracted from x-ray diffractogram data), material density, and chemical formula. The data was prepared by parameterizing the input data to

extract the key features from the material property data, then the data were normalized. Using the static permittivity values available in the database, the CNN was trained to predict permittivity. The prediction ability of the trained CNN was evaluated by comparison of the expected value to the predicted value for permittivity.

RESULTS

The CNN developed in this study was successful at predicting material permittivity based on the input parameters (crystal structure, density, and chemical formula). The material permittivity values from the database agreed well to the predicted values (R^2 = 0.9973). The prediction ability was further improved (R^2 = 0.9996) by tokenizing (a data preparation strategy) the chemical formulas that were used as training data.

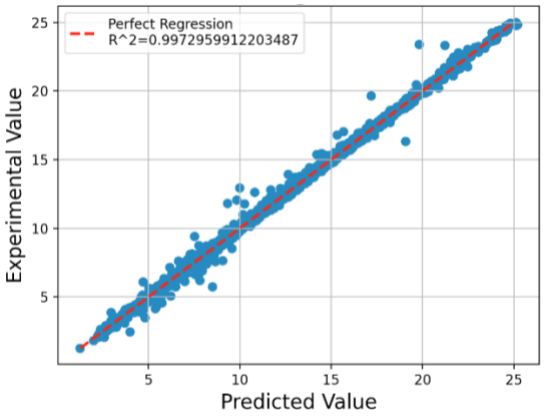

Figure 1. Experimental value vs predicted value of the convolutional neural network

DISCUSSION

The prediction network developed in this study demonstrates the feasibility of predicting dielectric permittivity from structural and compositional material parameters. As only static permittivity is available in the database used to train the model, its prediction is not directly applicable to frequency-dependent dielectric permittivity. By incorporation of frequency-dependent permittivity data, our future work will adapt this neural network to predict frequency-dependent permittivity.

CONCLUSION

The convolutional neural network developed in this work successfully predicts static dielectric constant of oxide materials from material physical and compositional input data. This work provides a baseline prediction network and its capability will be extended to prediction of microwave-frequency dielectric permittivity.

This work was performed in support of the US Department of Energy's Fossil Energy Crosscutting Technology Research Program. The Research was executed through the NETL Research and Innovation Center's Advanced Reaction Systems. Research performed by Leidos Research Support Team staff was conducted under the RSS contract 89243318CFE000003.

This work was funded by the Department of Energy, National Energy Technology Laboratory, an agency of the United States Government, through a support contract with Leidos Research Support Team (LRST). Neither the United States Government nor any agency thereof, nor any of their employees, nor LRST, nor any of their employees, makes any warranty, expressed or implied, or assumes any legal liability or responsibility for the accuracy, completeness, or usefulness of any information, apparatus, product, or process disclosed, or represents that its use would not infringe privately owned rights. Reference herein to any specific commercial product, process, or service by trade name, trademark, manufacturer, or otherwise, does not necessarily constitute or imply its endorsement, recommendation, or favoring by the United States Government or any agency thereof. The views and opinions of authors expressed herein do not necessarily state or reflect those of the United States Government or any agency thereof.

Microwave Dielectric Properties of Marinated Chicken Breast Meat

Samir Trabelsi

Quality and Safety Assessment Research Unit, U.S. National Poultry Research Center, 950 College Station Rd., Athens, GA, USA

Keywords: Marinated chicken meat, coaxial-line probe, microwave frequencies, dielectric properties

INTRODUCTION

Chicken meat constitutes one of the main inexpensive sources of proteins. Therefore, there has been a steady increase in both demand and consumption of chicken meat. Monitoring and assessment of the quality of chicken meat at the processing plant and selling outlets require the development of new tools for on-line implementation. Microwave dielectric-based methods and sensors are suitable for real-time in-line measurements since chicken meat is 70% water by composition [1]. The first step for the development of such methods and sensors is accurate measurement of the dielectric properties and the development of models correlating these properties with the quality attributes of interest including water holding capacity, freshness, and texture [1], [2]. In the United States, half of the raw poultry meat is marinated to increase water holding capacity and cook yield [2]. Therefore, in this study and for purpose of comparison, dielectric properties of non-marinated and marinated chicken breast meat were measured with a coaxial line probe at microwave frequencies between 0.2 GHz and 20 GHz at a room temperature of 22 ºC.

METHODOLOGY

Measurements over a wide frequency range allow a better understanding of the dielectric behavior of a given material. In this instance, with chicken meat composed of nearly 70% of water, the open-ended coaxial line measurement technique was selected. For dielectric properties measurements, for each chicken breast, the core taken out of the right side of the butterfly chicken breast was inserted into a stainless steel cup which was 19 mm in diameter and 19 mm in depth (Figure 1), and the dielectric properties were measured with a Hewlett-Packard 85070B[1] open-ended coaxial-line probe connected through an e-calibration module (Agilent Technologies N4639-60001) and a high-quality coaxial cable to a vector network analyzer (Agilent Technologies PNA-L N5230C) (Figure 2). The open-ended probe was calibrated with measurements on air, a short-circuit stainless steel block, and glass-distilled water at 25 ºC. Settings were made to provide measurements at 201

[1] Mention of trade names or commercial products in this publication is solely for the purpose of providing specific information and does not imply recommendation or endorsement by the U. S. Department of Agriculture

frequencies on a logarithmic scale between 200 MHz and 20 GHz. The open-ended coaxial-line probe came in firm contact with the chicken breast meat. Measurements were performed at a temperature of 22 °C. For the marination, a marinade solution was prepared. It consists of 91% distilled water, 6% sodium chloride, and 3% sodium triple polyphosphate. Marinade pick up percentage was calculated as follows:

Marinade pick up % = [(Marinated weight – Raw weight)/Raw weight]

Dielectric properties were measured for chicken breast meat with marinade pick up of 5%, 10%, and 15%.

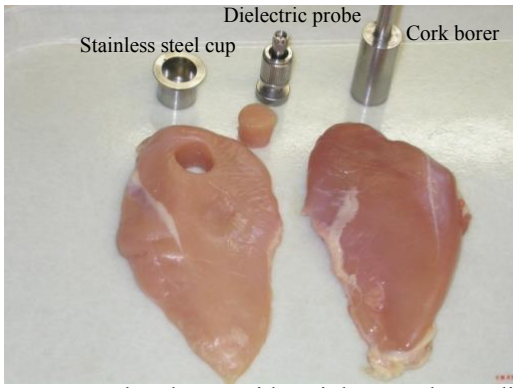

Figure 1. Chicken meat samples shown with stainless steel cup, dielectric probe, and cylindrical cutter.

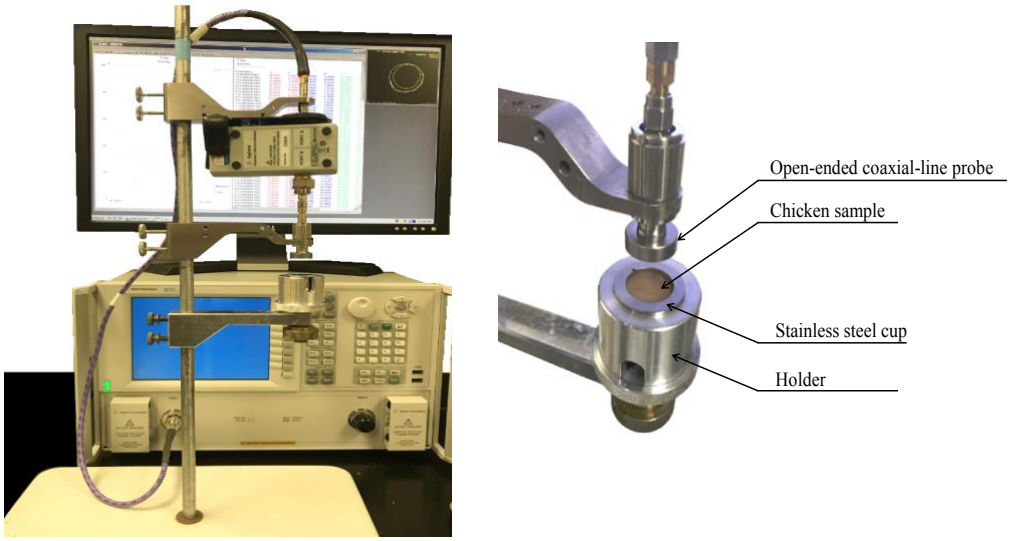

Figure 2. Measurement arrangement and close-up view of the open-ended coaxial line probe.

RESULTS

Figure 3 shows the dielectric properties of non-marinated and marinated chicken as a function of frequency. Overall, the dielectric properties decreased with frequency and increased with marination pick up. The dielectric constant shows a slope change at 4 GHz which can be attributed to water relaxation and the higher values of dielectric loss factor are attributed to ionic conduction. Differences in the dielectric response of non-marinated and marinated chicken breast meat are more significant for the dielectric loss factor and show distinctly the three levels of marination, especially in the lower region of the spectrum. At higher frequencies, above 6 GHz, the dielectric properties of non-marinated and marinated chicken breast meat are nearly superimposed.

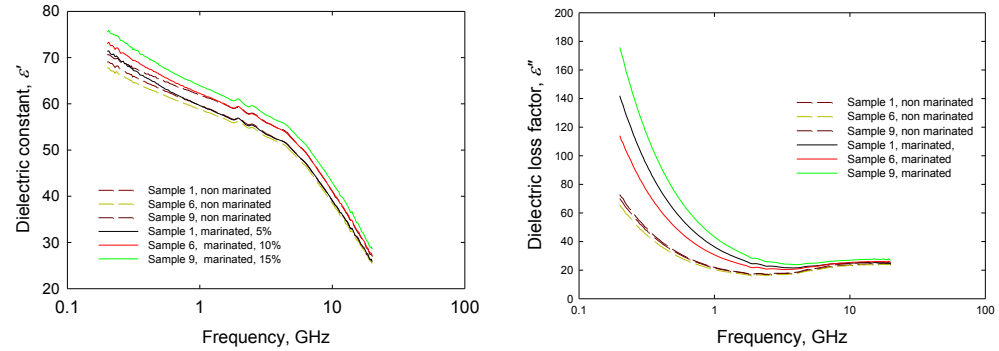

(a) (b)

Figure 3. Dielectric properties of non-marinated and marinated chicken breast meat measured at between 0.2 GHz and 20 GHz at 22 °C: (a) Dielectric constant, (b) Dielectric loss factor. Samples 1, 6, and 9 have a marination pick up percentage of 5, 10, and 15, respectively.

CONCLUSION

Dielectric data of marinated and non-marinated chicken meat over a broad frequency range from 200 MHz and 20 GHz were measured with an open-ended coaxial line. This will be instrumental in understanding their dielectric behaviors and developing methods and sensors for their nondestructive and instantaneous characterization. Here, the sensitivity of the dielectric properties to marinade pick up indicates it can be used to monitor this process in real time.

REFERENCES

[1] S. Trabelsi, Measuring changes in radio-frequency dielectric properties of chicken meat during storage, *J. of Food Measurement and Characterization*, 2018, **12**, pp. 683–690.

[2] D. Samuel, and S. Trabelsi, Influence of color on dielectric properties of marinated poultry breast meat *Poultry Science*, 2012, **91**, pp. 2011–2016.

Industrial Microwave Heating and the Industrial Internet of Things (IIoT): Exploration of Technology and Business Opportunities

Matthew Krieger

Cober Inc., Stratford, CT, USA

Keywords: Industrial Heating Industrial Internet of Things IIoT Telemetry

ABSTRACT

The Industrial Internet of Things (IIoT) [1] refers to the set of Internet-connected industrial systems including sensors, programmable logic controllers (PLC), factory machines and other interconnected devices. The connectivity of these devices creates opportunities for real time data collection and analysis which can provide substantial positive business impacts including costs savings, increases in productivity and ultimately a higher quality end-product. This presentation will explore IIoT technologies in general, describe usage scenarios within the industrial microwave heating and process heating areas and explain resulting business opportunities.

The terminology around IIoT technologies will be defined and explored. Usage scenarios for IIoT in industrial microwave heating applications will be described. Several real-world implementations will be covered, along with a set of business benefits that can be realized from implementations of IIoT and data collection technologies. The following serves as a tentative outline of covered topics:

- Industrial Internet of Things (IIoT) definition
- Definition of related technologies
- Exploration of generalized IIoT implementations
- Examples of IIoT telemetry related to industrial microwave applications
- Business opportunities in the industrial microwave heating area

REFERENCES

[1] Industrial Internet of Things, *Wikipedia*, https://en.wikipedia.org/wiki/Industrial_internet_of_things

Effect of Dynamic Changing Frequency on the Microwave Heating Uniformity of Food in a Solid-State System

Ran Yang, Jiajia Chen

Department of Food Science, University of Tennessee, Knoxville, TN, USA

Keywords: microwave heating, uniformity, solid-state, frequency shifting algorithm

INTRODUCTION

Non-uniform heating in magnetron-based domestic microwave ovens has been a great concern since it lowers the food quality and leads to safety problems. The recent development of solid-state microwave power source has a great potential to replace the magnetron-based power source to deliver heat more uniformly. The precious control of the microwave parameters of power, frequency, and phase allows dynamic interactions between microwave and food. Korpas et al. developed a customized frequency and phase-shift efficiency optimization algorithm based on computer simulation, which can be used to control microwave parameters for improving power efficiency [1]. It was also reported that shifting the frequency orderly could improve the heating uniformity [2]. In reality, the dynamic control of microwave parameters is a complicated process because various combinations of shifting step, rate, and order could influence the microwave heating performance. Instead of utilizing all possible microwave parameters, parameter combinations can be optimized based on their complementary performance to deliver better heating performance. This study aimed to evaluate the effect of different frequency-shiting strategies on microwave heating uniformity.

METHODOLOGY

A solid-state microwave system comprised of a generator (PA-2400-2500MHz-200W-4, Junze Technology) and a domestic microwave oven cavity (Panasonic Model NN-SN936W) was used in this study. The system has four 200 W ports, and only one was used to focus on the effect of single port frequency in this study. A tray of model food was made with 1% gellan gum (Kelcogel, Kelco Division of Merck and Co., San Diego, CA), 0.17% $CaCl_2$, and deionized water. The model foods were placed at the center of the oven turntable and heated without rotation from 0 °C for 6 minutes. The top surface temperatures were recorded with a thermal camera (FLIR C3, Boston, MA) and analyzed by FLIR Tools (2020 © FLIR® Systems, Inc.). The heating uniformity index (HUI) was evaluated by the ratio of standard deviation and average temperature increase.

Different frequency-shifting strategies were evaluated: 1) constant-frequency (from 2.40 to 2.47 GHz with a step size of 0.01 GHz); 2) orderly (incremental and decremental) shifting-frequency at different shifting rates of 45 and 15 s (Figure 1A); and 3)complementary shifting-frequency strategy at different shifting rates of 45 and 15 s (Figure 1B). In this study, the frequency higher than 2.47 GHz was not used because of the high refection power and low microwave efficiency.

The complmentary frequency-shifting strategy (Figure 1B) was designed following a customized algorithm (Figure 2) that used constant-frequency heating results to identify complementary frequency combinations to achieve the best uniformity.

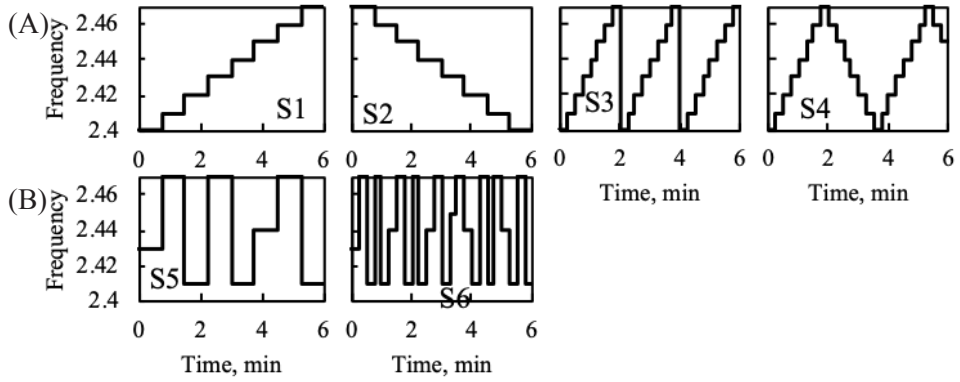

Figure 1 Dynamic change of frequency. (A) S1: 45s-incremental, S2: 45s-decremental, S3: 15s-incremental, S4: 15s-mixed shifting (B) S5: 45s-complementary, S6: 15s-complementary shifting.

Input: 1. Pre-collected temperature profiles (6 min 200W) for single frequency (2.40 to 2.47 GHz), t_n

2. Desired steps of frequency-shifting, N

Output: A group of frequency in optimized order, $\{\boldsymbol{P_N}\}$

Initialization:

The single frequency with minimal HUI as f_1, corresponding temperature profile as T_1

$T_{old} = T_1$, n = 1

while n < N, n ⟵n + 1

  for i = 1 to 8

    $T_{updated,i} = T_{old} + t_i$

    $HUI_{updated,i} = std_{T,updated,i}/\Delta ave_{T,updated,i}$

  end for

  $i_{optimal}$ ⟵ i for $(HUI_{updated,i})_{mini}$

  $T_{old} \longleftarrow T_{updated,i,optimal}$

  $\{\boldsymbol{P_N}\} \longleftarrow f_{i,optimal}$

end while

Figure 2 Algorithm to determine the complementary shifting-frequency strategy

RESULTS

When heating at constant-frequency, the heating uniformity varied considerably. The best and worst heating uniformity was observed at 2.43 and 2.46 GHz, respectively (Figure 3A). The locations of hot and cold spots also changed considerably with frequency change. The hot and cold spot location variations were utilized and developed as a complementary frequency-shifting strategy. Both the orderly shifting and the complementary shifting strategies showed better uniformity than all the constant-frequency scenarios (Figure 3B). The complementary shifting-frequency strategy also showed better uniformity than the orderly shifting strategy. While the shifting rates and orders of the frequencies made little difference to the heating results.

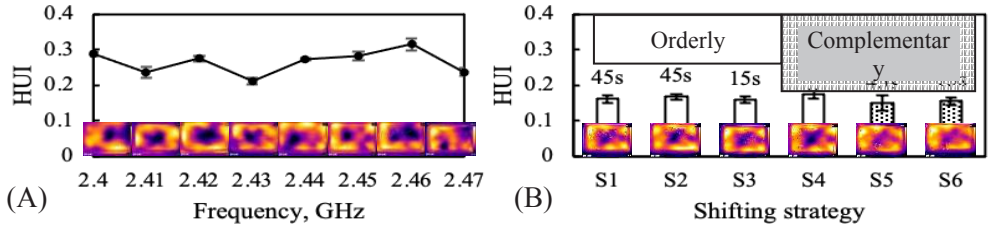

Figure 3 Heating uniformity index (HUI) after processing under various conditions for 6 min from 0°C.(A) Heating at constant-frequency (from 2.40 to 2.47 GHz);(B) Heating at shifting-frequency. All results are shown as the average of triplicate.

DISCUSSION

The frequency-shifting strategy could improve the heat distribution. The combination of several different frequencies within one heating scenario benefited from the complementary heating patterns generated by different frequencies, which contributed to a better heating uniformity. The orderly shifting strategy arbitrarily piled up all possible patterns, while the complementary shifting strategy can identify the most efficient way to combine the complementary frequencies for a more uniform heating.

CONCLUSION

Dynamic microwave frequency control strategies can improve the heating uniformity. The frequency-shifting strategies can be developed based on the complimentary heating performances of single frequencies.

REFERENCES

[1] Korpas, P., Wieckowski, A., & Krysicki, M. (2014). Effects of applying a frequency and phase-shift efficiency optimisation algorithm to a solid-state microwave oven. In *2014 20th International Conference on Microwaves, Radar and Wireless Communications (MIKON)* (pp. 1–4). IEEE.

[2] Du, Z., Wu, Z., Gan, W., Liu, G., Zhang, X., Liu, J., & Zeng, B. (2019). Multi-physics modeling and process simulation for a frequency-shifted solid-state source microwave oven. IEEE Access.

Computational Characterization of a Millimeter-Wave Heat Exchanger with AlN:Mo Cylindrical Susceptors

Catherine M. Hogan[1], Brad W. Hoff[2], Ian M. Rittersdorf[3], and Vadim V. Yakovlev[1]

[1]Department of Mathematical Sciences, Worcester Polytechnic Institute, Worcester, MA, USA
[2]Air Force Research Laboratory, Albuquerque, NM, USA
[3]Naval Research Laboratory, Washington, DC, USA

Keywords: Energy efficiency, multiphysics simulation, temperature field, power beaming.

INTRODUCTION

A new type of electromagnetic (EM) heat exchangers (HX) has been recently introduced for ground-to-ground millimeter-wave (MMW) power beaming applications [1]. It comprises an assembly of ceramic elements and a metal baseplate that contains channels with fluid flow. The EM power of the incident wave is dissipated in the ceramic elements and heats the baseplate and the fluid taking the heat away. Computational studies of the MMW HX with a susceptor as a single rectangular block of a ceramic composite (AlN:Mo) [2] have shown elevated energy efficiency and excellent uniformity of the temperature field. However, while these results further stimulated the development of the technology, the cost-effective production of the ceramic parts and practicality of use suggest a physical prototype of the MMW HX to use multiple cylindrical susceptors.

Here we present computational results demonstrating feasibility of the design of the experimental system made of five AlN:Mo cylinders on a square baseplate and compare it with the systems whose layouts are suggested by the highest density packing of equal circles in a square [3]. We show that, in the designs of different geometry, maximum energy efficiency can be achieved using the composites with different concentration of molybdenum, whereas all the considered materials provide excellent uniformity of temperature distribution within the ceramic cylinders.

METHODOLOGY

Computational experiments were conducted following the approach based on the coupled EM-thermal simulation and reported in [2]. The simulation was carried out with the finite-difference time-domain technique implemented in *QuickWave* [4]. The main model reproduces the prospective experimental system which consists of an array of five cylindrical susceptors on a thin metal plate and irradiated by a plane wave (95 GHz), as shown in Figure 1. The layout features an air gap between the points of cylinders' contacts that is required to accommodate thermal expansion of the ceramic material.

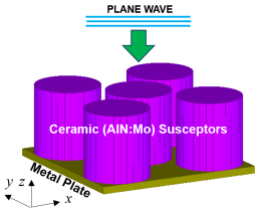

Figure 1. Model of the physical prototype; air gap between the contact points 1 mm.

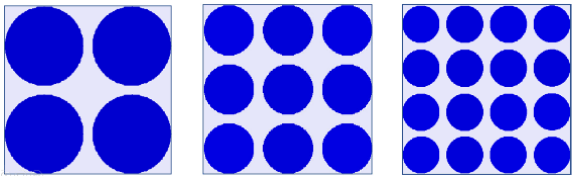

(a) (b) (c)

Figure 2. Layouts of cylinders in the packings of equal n circles in a square for $n = 4$ (a), $n = 9$ (b), and $n = 16$ (c) with 1 mm gap between the contact points.

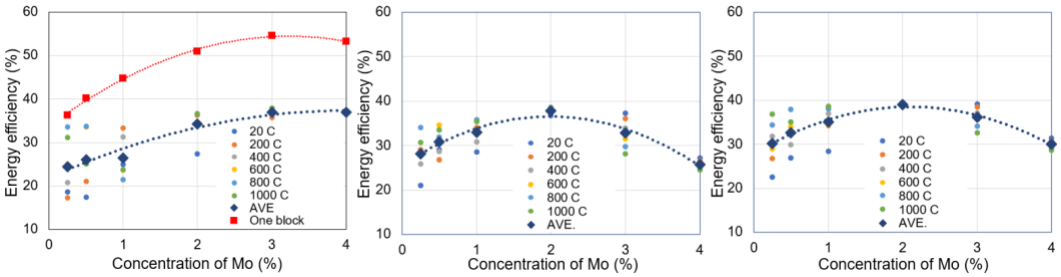

(a) (b) (c)

Figure 3. Energy efficiency (at different temperatures of the AlN:Mo composite and average) of the physical prototype (a) and the systems with four (Figure 2(a)) (b) and 9 (Figure 2(b)) (c) cylinders as functions of Mo contents; red points in (a) – the system with one rectangular block.

The susceptor is made of aluminum nitride (AlN) doped with molybdenum (Mo). Data on the materials with six different Mo concentrations from 0.25% to 4.0% (by volume) are detailed in [2] and includes temperature-dependent dielectric constants and the loss factors (at 95 GHz) as well as specific heats and thermal conductivities.

The design in Figure 1 has the ratio of the absorbing area to the area of the square baseplate as $d = 0.598$. This implies that the layout may cause lower energy efficiency (compared to a single susceptor [1]-[2] with $d = 1$). The problem on the packing of equal circles in a square [3] provides the highest value of d (0.785) for four, nine, and sixteen cylinders arranged in rows and columns. This suggests the layouts of the cylinders shown in Figure 2 as possible alternative designs. Additional models reproducing these three configurations were developed and employed for the comparative computational analysis.

RESULTS

EM simulation of the 5-cylinder model (radius 4.8 mm, height 10 mm, metal plate 24.4 × 24.4 mm) displays the highest energy efficiency (defined as ratio of the total absorbed power to the power of the incident field) when the cylinders are made of the composite with 3.0-4.0% Mo (Figure 3(a)). This is consistent with the results for the system with a single rectangular block [2], though here the efficiency is notably down. The graphs for both the 4- and 9-cylinder systems (Figure 3 (a), (b)) have maxima of average energy efficiency at about the same level, but for Mo = 2.0%.

Simulation of the temperature field induced in the ceramic composite by the incident MMW field shows that distribution of temperature along the z-axis is highly

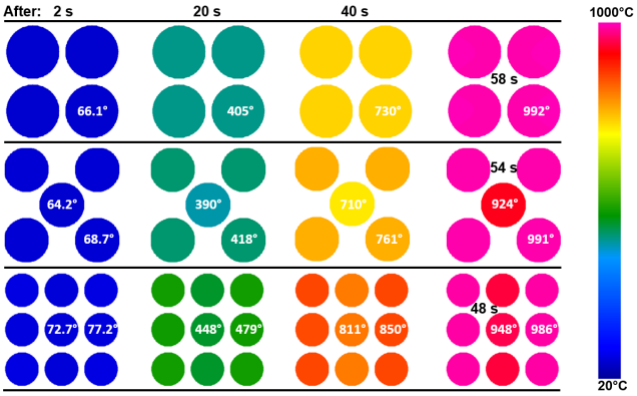

Figure 4. Simulated temperature field in the central cross-sections (the *xy*-plane) of the systems with n = 4, 5, and 9 and incoming power density 430, 357, and 394 W/mm^2, respectively; Mo = 3%.

uniform in all systems. Typical temperature patterns in the *xy*-plane are shown in Figure 4. In the 4-cylinder model, the temperature distribution is most consistent: all cylinders are heated at about the same rate with very similar patterns. In the systems with higher n, the central cylinder is heated slower and at the final stage its maximum temperature can be lower by 40-60ºC. While the 4-cylinder system takes the longest to reach 1,000ºC, the delay is only 10 s in comparison with the 9-cylinder system, which is the fastest.

DISCUSSION AND CONCLUSION

As the models with four, nine, and sixteen cylinders were selected due to their high densities in the circles in a square packing problem [3], their densities with the 1 mm gap turned out to be 0.722, 0.662, and 0.605, respectively. Despite these higher densities, the energy efficiency of the tested models is about the same as the 5-cylinder model (0.598). The energy efficiency of all considered scenarios drops significantly when compared to the single rectangular model (54 to 37%). For the 5-cylinder system, energy efficiency is at its maximum when the material has 3.0-4.0% Mo, while the 4 and 9 cylinders displayed their maxima at 2.0%. Satisfactory uniformity of temperature distribution in the cross-sectional plane is seen in all the layouts and all the materials.

REFERENCES

[1] B.W. Hoff, M.S. Hilario, B. Jawdat, A.E. Baros, F.W. Dynys, J.A. Mackey, V.V. Yakovlev, C.E. Andraka, K.M. Armijo, E. Savrun, and I.M. Rittersdort, Millimeter wave interactions with high temperature materials and their applications to power beaming, *Proc. 52nd IMPI's Microwave Power Symp. (Long Beach, CA, June 2018)*, pp. 82-83.

[2] P. Kumi, S.A. Martin, V.V. Yakovlev, M.S. Hilario, B.W. Hoff, and I.M. Rittersdorf, Electromagnetic-thermal model of a millimeter-wave heat exchanger based on an AlN:Mo susceptor, *COMPEL*, vol. 39, no. 2, pp. 481-496, 2020.

[3] M. Goldberg, The packing of equal circles in a square, *Mathematics Magazine*, vol. 43, no. 1, pp. 24-30, 1970.

[4] *QuickWave*, 1998-2019, QWED Sp. z o.o., www.qwed.com.pl.

Green Gel Synthesis of Microwave-induced Plasma-in-liquid (MPL) and its Application for On-site Water Treatment

S. Horikoshi

Sophia University, Dept. of Material and Life Science, Tokyo, Japan

Keywords: Gel, microwave, in-liquid plasma, wastewater treatment, radioactive material

INTRODUCTION

In-liquid plasma refers to plasma generated in water and is a new technology for which both fundamental and applied research is being pursued. DC and AC power supplies, lasers, microwaves, and RF are used as plasma generating sources, but microwaves can generate plasma without using an aqueous electrolyte solution. These are expected to be used for various purposes [1]. Generally, microwave-induced plasma-in-liquid (MPL) cannot be used practically because if plasma is generated for several seconds, the tip of the electrode is melted and crushed. We accidentally discovered that the deterioration of the electrodes did not progress. The plasma in the liquid could operate stably for a long time, when the microwave irradiation is pulsed using a semiconductor microwave generator. We have confirmed that this device can be used to decompose non-degradable substances in water, within a several minutes.

As a test chemical reaction using MPL, we focused on nanoparticle synthesis and conducted experiments. Unfortunately, only poor-quality nanoparticles were produced, but it was discovered that the polymer, which was added as a protective agent for the nanoparticles, becomes a gel without adding an organic solvent, a cross-linking agent, or an initiator. In this study, we focus on the gelation of polymers by MPL, elucidating the mechanism involved. This gel was generated in wastewater, and water treatment was performed using both MPL decomposition and gel adsorption recovery.

METHODOLOGY

The MPL device uses a semiconductor-type 2.45 GHz microwave oscillator (LeanFa GEAP-A003A01 or Ampleon M2A-R) that can strictly control pulses and uses a waveguide to insert the tungsten antenna electrode into an aqueous solution in a cylindrical

quartz reactor. It is configured to irradiate microwaves (Figure 1). The microwaves are concentrated at the tip of the electrode, and a ceramic spacer is provided at the junction between the antenna and the waveguide to provide insulation and diffusion of heat generated by plasma. Since microwave irradiation prevents the deterioration of the electrodes, due to the heat of the plasma, pulse irradiation was performed, and the pulse conditions were similar to a previous study [2]. Optimal pulse conditions were a microwave irradiation power of 150 W (pulse amplitude), a pulse period of 16.7 ms and a pulse width of 13.36 ms.

An aqueous solution containing inorganic ions such as iodine, nickel, cesium, and copper (1~100 ppm) is used as model wastewater, and the gel is polyvinylpyrrolidone (PVP) or sodium polyacrylate (PAA-Na). Pulsed microwave was irradiated to generate plasma in this aqueous solution. After irradiation of MPL, the generated PVP gel was recovered from the drain valve together with the aqueous solution.

Dynamic light scattering and fully automatic elemental analyzer were used (Otsuka Electronics Co., Ltd., DLS, ELSZ-2000ZS and Perkin Elmer Co., Ltd., PE2400 Series II CHNS/O). Fourier transform infrared spectroscopy (FT-IR, JASCO Co., FT/IR-4600), Raman spectrophotometer (NRS-4500) and UV/Vis (V-760) absorption spectrum were used. Nuclear magnetic resonance (NMR) spectroscopy was measured by JEOL Ltd. Lambda 500 MHz, which was used to measure ^{13}C-NMR and ^{1}H-NMR. The NMR data analysis system were used with a JEOL Ltd. ALICE. X-ray photoelectron spectroscopy (XPS) and scanning electron microscope (SEM) were used (ULVAC-Phi ESCA 5800ci and a Hitachi High Technologies Co., Ltd., SEM, SU8000). A Toki Sangyo Co., Ltd. viscometer (R215) was used to measure the viscosity of the gel.

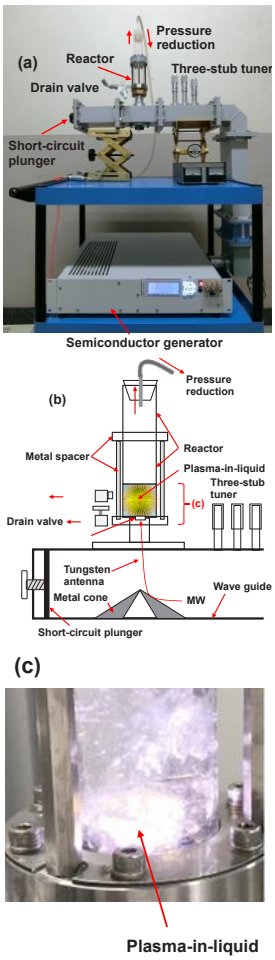

Figure 1. (a) Photograph and (b) illustration of MPL devices; (c) photograph of generated in-liquid plasma.

RESULTS & DISCUSSION

A PVP gel was formed by irradiating an aqueous solution of polyvinylpyrrolidone (PVP) (0.1 g mL^{-1}) for 5 min with MPL. To elucidate the gel formation mechanism, FT-IR of PVP, before and after MPL irradiation, was measured. From the FT-IR spectrum, peaks around 1300 and 1650 cm^{-1} were confirmed in both PVP before and after irradiation, suggesting that the tertiary amide group was contained even after gelling. Next, using N-methylpyrrolidone (NMP), which is a monomer of PVP, as a model, structural changes before and after in-liquid plasma irradiation were analyzed by ^{13}C-NMR. Before irradiation, one amide bond peak was observed around 180 ppm, but irradiation increased the number of peaks to five. This suggests that the amide bond of NMP and the amide bond

of the PVP gel precursor are different. In addition, from the emission spectrum generated from the plasma in the solution, it was predicted that the active species that contributed to the chemical reaction was •OH. From these results, in the early stage of synthesis, the five-membered ring in the PVP structure is opened by the attacking •OH (confirmed by molecular orbital calculation), and a radical intermediate is generated. It is considered that these radical intermediates formed new amide bonds, and by repeating this, a three-dimensional gel structure was formed (Figure 2).

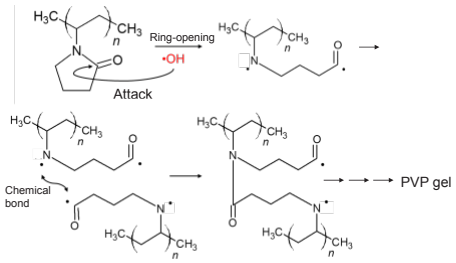

Figure 2. Mechanism of PVP-gel synthesized by using MPL.

Ionic contaminant recovery in water with PVP-gel resulted in only 15-65 % recovery. Therefore, the polymer was changed to PAA-Na for ion removal testing. PAA-Na was added to an aqueous solution in which copper ions were dissolved, and plasma irradiation was performed in the solution to recover the copper ions. Irradiation with 150 W microwave generated in-liquid plasma occurred for 30 sec. It was observed that the turquoise color of copper ions was wrapped in the gel as the gel was formed. When the copper ion concentration of the supernatant aqueous solution was measured, it was found that 98% of the copper ions were removed (Figure 3).

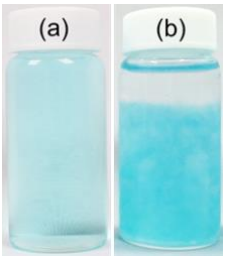

Figure 3. Photographs of aqueous solution containing Cu ions and PAA-Na (a) before and (b) after plasma irradiation in the liquid (inclusion of copper ions by gel).

On the other hand, in the adsorption removal experiment using PAA-Na gel synthesized by MPL, the adsorption of Cu ions was about 100%, tin (Sn) ions were 69.9%, and lead (Pb) ions were 53.1%.

CONCLUSION

Gels are often used as a technique for removing ionic contaminants in water. However, if the dried gel is put in contaminated water, the gel will not swell if there is not enough water, and it cannot be used. On the other hand, gel synthesis can be a chemical reaction in water. However, most gelling agents are highly toxic. Therefore, when used in water treatment, they can result in secondary pollution. The gel synthesized in this study is a new method that can treat a small amount of contaminated water without causing secondary pollution because it creates a cross-linked gel by the power of electricity without using any gelling agent.

REFERENCES

[1] S. Horikoshi, N. Serpone, *RSC Adv.*, **7**, pp. 47196–47218, 2017.
[2] S. Horikoshi, S. Sawada, S. Sato, N. Serpone, *Plasma Chem. Plasma Process.*, **39**, pp. 51–62, 2019.

Effect on the Microstructure of the Dietary Fiber of Bagasse and Sugarcane Bud using an Alkaline Treatment with Microwave-assisted Sodium Hydroxide

María Elena Sánchez-Pardo[1], D. I. Llanes Gil-López[2,3], J. A. Lois-Correa[2]

[1]Instituto Politécnico Nacional, ENCB-Zacatenco, Av. Wilfrido Massieu, 07728, Ciudad de México, México.
[2]Instituto Politécnico Nacional, CICATA-Altamira, km 14.5 carretera Tampico–Puerto Industria Altamira, Tamps., México, 89600
[3]Tecnológico Nacional de México, Instituto Tecnológico de Altamira, Tampico, Tamps.
*Autor correspondencia: alimentoselena@hotmail.com

Keywords: microstructure, microwave, fiber, sugar cane bagasse.

INTRODUCTION

Sugarcane bagasse is a by-product of sugar milling; it consists of particles of different sizes whose average size is 2.5 mm. The granulomere of bagasse depends on the work of the sugarcane preparation equipment and to a lesser extent on the design of the mills and the variety of the sugarcane. Fiber has been designated as the water insoluble, solid organic fraction, present in the stem of sugar cane. It is characterized by its marked heterogeneity (hemicellulose, lignin, cellulose). The soluble solids are mainly composed of sucrose, as well as other chemical components such as wax, but to a lesser extent. The water in the bagasse is retained through absorption and capillarity mechanisms. This phenomenon plays a very important role in some processes. The bud is the most tender part of the cane plant. It is the upper portion of the stem, with two or three internodes with vegetative buds (commonly used as seed by farmers) and the leaves or palm. The bud contains the greatest amount of reducing sugars, fiber, protein and ethereal extract [1].

Rapid microwave heating ruptures the walls and structures such as cellulose, hemicellulose and lignin; the dissolution of these complexes favors the use of fibers for human consumption. In the case of solutions whose molecules do not have an intrinsic dipole moment (e.g. NaOH), the electric field of the incident microwave has sufficiently high intensity to generate dipole moments and force the spinning movement of such molecules. The result of this interaction is similar to the previous case, where a large amount of heat is dissipated into the sample [2].

METHODOLOGY

The sugarcane bagasse was provided by the "Ingenio de Ciudad de Panuco" SAPI S.A. de C.V., which was received with an approximate humidity of 40%. For this reason it was dried in a vertical dehydrator with forced air and ground in a mill blades to obtain a particle size of the order of microns passing through a 250 μm mesh, in order to comply with the standards for the generation of flours for use in food. The bud was collected from the field, in conjunction with an association of cattle ranchers, which is in the city of Ozuluama, Veracruz, in the north of this state.

Microwave-assisted alkaline treatment is emerging as a novel waste treatment for the first time, using alkaline agents in combination with microwaves. In this sense, experiments were carried out with different amounts of the alkaline agent sodium hydroxide (NaOH) to optimize the method by adapting this parameter due to the high hygroscopicity of sugarcane bagasse. Experiments were carried out with 30 mL, 45 mL, 60 mL, and 75 mL of NaOH, respectively, using the average power (600 Watts) of a household microwave frequency of 2400 MHz. The rationale for this treatment was that the heating of the interstitial water in the sample distends its cells and leading to the rupture of its glands and material receptacles, promoting hemicellulose and lignin bond breaking. After the reaction time, the fibers were washed with distilled water until the latter's pH equalized. A microscopic analysis was carried out with Scanning Electron Microscopy (SEM) of the fibrous residues to have a reference standard before applying the alkaline agent (Fig. 1).

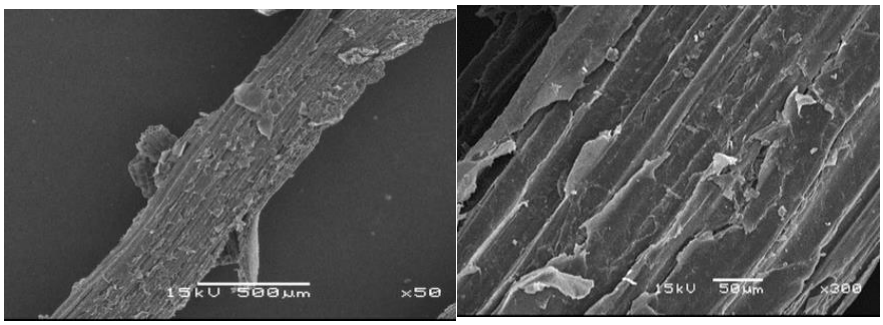

Figure 1. Micrograph with SEM of Cane Bagasse without treatment a) 50X magnification b) 300X magnification.

RESULTS

In the chemical analysis of the untreated residues, the high fiber content in both cases, which for this work is desirable if the lignin is depolymerized, for these residues, to be able to give a contribution of nutritional fiber to food for humans. On the other hand, in Figure 2, the fully lignified walls, and are observed due to the lignocellulosic matrix [3]. From the dietary fiber analysis results on bagasse treated with different volumes of alkaline solution, a proportional relationship can be found between increasing solution concentration and decreases in the dietary fiber, with the lowest value of dietary fiber being the experiment with 75 mL of the agent. Chemical changes were observed, highlighting the decrease in

dietary fiber, achieving reductions of 27.95% for bagasse and 33.3% for the bud, both with alkaline treatment using 75 mL of alkaline agent.

DISCUSSION

From the dietary fiber results, microwave irradiation's positive effect can be glimpsed since lower fiber values were obtained in the experiment to which microwave energy was applied compared to the control. Improvements of 4.0 and 5.0% for the bagasse and sugar cane bud experiments, respectively, were observed. Microscopies show bagasse fibers' images and bud alkaline treated with microwave-assisted 2% NaOH. In Figure 2 (a), the fibers are simultaneously cracked in the walls. There are fibers with bends because the fiber bundles are not packed and have more flexibility due to the alkaline agent's action. In Figure 2 (b), a significant fractionation of the sugarcane bud's fibers is observed due to the depolymerization of lignin and the breaking of bonds [4].

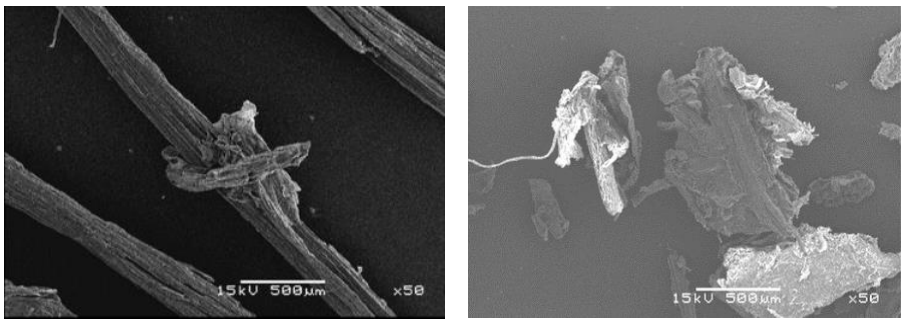

Figure 2. Bagasse (a) and sugarcane bud (b) treated alkaline with 2% NaOH assisted by microwave. Magnification 50 X.

CONCLUSION

The microwave-assisted alkaline treatment produced physical changes in the treated fibers. Due to the lignin bonds' breakdown, the formation of accumulations in the treated fibers was also observed. It is possible to use these delignified fibers as dietary fiber in food for human consumption.

REFERENCES

[1]C. Gastón, R. Bambanaste, J. Lois, G. Alfonso and M. Herryman. 1982. Subproductos de caña de azúcar. ICIDCA. Capitulo 2, Habana, Cuba.

[2]D. I. LlanesGil-López, J.A.Lois-Correa, M.E.Sánchez-Pardo, M.A. Domínguez-Crespo, A.M.Torres-Huerta, A.E.Rodríguez-Salazarc and V.N.Orta-Guzmán. 2019. Production of dietary fibers from sugarcane bagasse and sugarcane tops using microwave-assisted alkaline treatments. Industrial Crops and Products. 135(1) Pages 159-169. https://doi.org/10.1016/j.indcrop.2019.04.042

[3]E. Ziger and L. Taiz. 2007. Fisiología Vegetal. Publicaciones Universidad Jayme, pág. 291

[4]X. Weihua, H. Lujia, Z. Yanyan. Comparative study of conventional and microwave-assisted liquefaction of corn stover in ethylene glicol, *Industrial Crops and Products 34* (2011) pp. 1602–1606.

Waste Processing Using Microwave Assisted Pyrolysis

Scarlett Allende[1], Raviteja Challa[1], Graham Brodie[1,2], Mohan V. Jacob[*1]

[1]Electronics Material Lab, College of Science and Engineering, James Cook University, Townsville QLD 4811 Australia
[2] Dookie Campus, The University of Melbourne, 940 Nalinga Rd., Dookie, 3647, Australia
Correspondence Email: Mohan.Jacob@jcu.edu.au

Keywords: Microwave Pyrolysis, Domestic Waste, Urban Waste, Biomass, Bioenergy

INTRODUCTION

Population and economic growth have produced an increase in energy consumption, and domestic and urban waste. The disposal of solid waste has become a significant environmental issue due to greenhouse emissions [1], [2], [3], [4]. Principally, Municipal Solid Waste (MSW) represents a high waste generation in Queensland (3.3 tonnes/year per capita) [5], which includes food and non-organic produce (29 %) and residues (21%), respectively [6]. Although part of these wastes will disintegrate and decompose into the soil within months, some wastes can stay in landscape for long periods. Proper utilisation and management of waste could generate income through resource recovery and avoid environmental hazards. As an example, conversion of solid waste into by-products, using microwave pyrolysis, will be a sustainable approach to generate energy. This research involves the breakdown of domestic waste using microwave pyrolysis for energy yield optimization of its by-products.

METHODOLOGY

There are two central parts of this research using food waste as the feedstock for the microwave pyrolysis, with the focus on obtaining the maximum by-product yield from the by-products. The first stage involves feedstock analysis, mainly focusing on physical-chemical aspects, such as, elemental composition and high heating value. Once the biomass analysis is completed, the biomass is pyrolysed under controlled parameters, like microwave susceptor addition (%) and microwave power (kW). The operational conditions, such as the amount of susceptor, power and time allowed for optimising the by-product yield (biogas, bio-oil, and biochar), were evaluated. The bio-oil and biogas will be characterised using gas chromatography-mass spectrometer (GC-MS), and biochar will be analysed using thermogravimetric analysis.

The microwave pyrolysis system comprises a computer-controlled microwave generator, automatic tuner, chamber, condensers, and a vacuum pump. Nitrogen gas is used

to maintain an oxygen-free atmosphere during the experiments. Microwave power is delivered by a computer-controlled automated system. Once the system is loaded with the biomass, the air is removed from the system using the rotary vacuum pump and is purged with nitrogen gas.

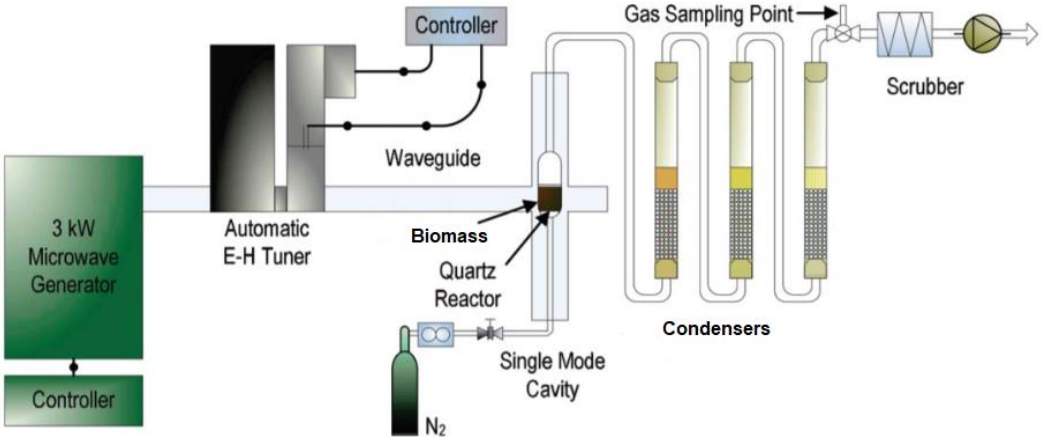

Figure 1. Microwave pyrolysis system [7].

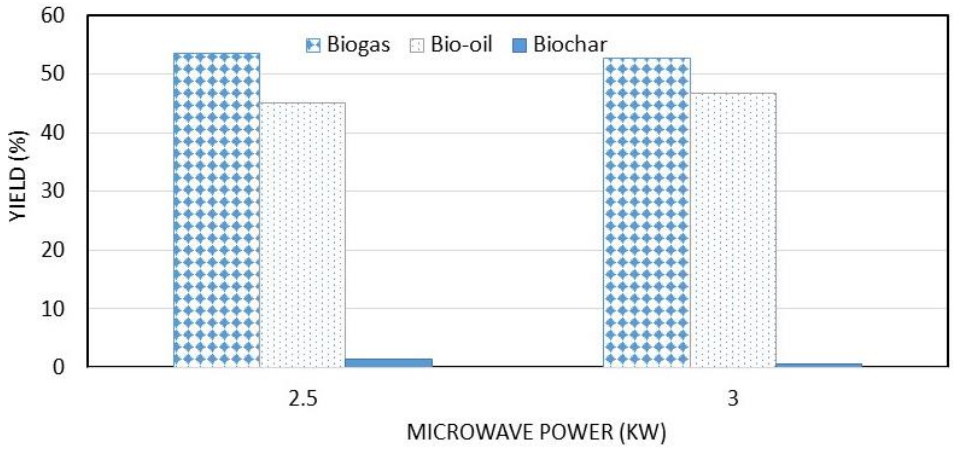

Figure 2. By-product yield optimisation from the breakdown of domestic food waste using microwave pyrolysis.

RESULTS

Figure 2 shows the by-products yield optimisation generated in the microwave pyrolysis process. Biomass used in the experimental procedure was food residues (approximately 180g of domestic waste mixed with 15% bio-char, which is used as a

Microwave susceptor. The applied treatment time was 30 minutes at two different microwave power levels (2.5 and 3kW).

DISCUSSION

By-product yield is affected by microwave power (kW) and susceptor percentage. High power level (3kW) and char addition (15%) produces high biogas yield. In contrast, low biochar yield is generated at high microwave power (above 1 kW) and reaction time. High power and microwave susceptor increased the heating rates during the conversion process, promoting a faster volatiles formation, and improved gas fraction production due to higher thermal cracking. Low microwave power produced less bio-oil because the low temperatures yield lower volatile generation.

CONCLUSION

The energy yield of the by-products, generated from the urban waste breakdown, is optimised, considering the operational conditions of the microwave pyrolysis process. Detailed data and analysis will be presented during the conference.

ACKNOWLEDGEMENTS

SA acknowledges the RTP scholarship.

REFERENCES

[1] H. Liu, X. Ma, L. LiZhi, F. Hu, P.Guo and Y. Jiang, "The catalytic pyrolysis of food waste by microwave heating," *Bioresource Technology,* vol. 166, pp. 45-50, 2014.

[2] D.Czajczyńska, L.Anguilano, H.Ghazal, R.Krzyżyńska, A.J.Reynolds, N.Spencer and H.Jouhara, "Potential of pyrolysis processes in the waste management sector," *Thermal Science and Engineering Progress,* vol. 3, pp. 171-197, 2017.

[3] F. Yang, G. Li, Q. Yang and W.H.Luo, "Effect of bulking agents on maturity and gaseous emissions during kitchen waste composting," *Chemosphere,* vol. 93, no. 7, pp. 1393-1399, 2013.

[4] M. N. Mahamad, M. A. A. Zaini and Z. A. Zakaria, "Preparation and characterization of activated carbon from pineapple waste biomass for dye removal," *International Biodeterioration & Biodegradation,* vol. 102, pp. 274-280, 2015.

[5] M. Ritchie, The state of waste in Australia – a 2019 review," Insidewaste, 14 August 2019. [Online]. Available: https://www.insidewaste.com.au/index.php/2019/08/14/a-review-of-the-state-of-waste-in-australia-in-2019/. [Data uzyskania dostępu: 22 January 2021].

[6] Australian Biomass for Bioenergy Assessment, „Queensland technical methods - Urban waste," Australian Biomass for Bioenergy Assessment (ABBA), 2018.

[7] J. P. Robinson, S. W. Kingman, R. Barranco, C. E. Snape and a. H. Al-Sayegh, "Microwave Pyrolysis of Wood Pellets," *Ind. Eng. Chem. Res,* vol. 49, p. 459–463, 2010.

Use of Novel Microwave Technology as a Hurdle Antimicrobial Intervention to Decontaminate Salmonella spp. in Chicken Breast

Darvin Cuellar[1], Don Stull[2], and Alejandro Echeverry[1]

[1]Texas Tech University, Lubbock, USA

[2]MicroZap, Lubbock, USA

INTRODUCTION

Chicken is the most consumed meat in the United States with a per capita consumption of 48.8 kg. Chicken meat is considered a healthy source of protein and it is preferred over red meat because its lower fat and cholesterol content [2]. The current market for chicken concentrates on more convenient and nutritive products such as deboned and deskinned chicken parts, marinated chicken, patties, nuggets, etc., yet it can also be a good media for microorganisms to grow, including pathogenic bacteria such as *Salmonella* spp. From 1998 to 2017 there were 298 chicken-related *Salmonella* outbreaks, resulting in 905 hospitalizations and 4 deaths [1]. For this reason, it is important the development of new antimicrobial interventions and processes that together can help to eliminate *Salmonella* spp. in fresh (raw) chicken. Microwaves are commonly used to heat and cook foods but also studies have proven that the technology can be used to "pasteurize" foods using it at low temperatures without cooking said foods. In this study we evaluate the potential of microwaves to decontaminate chicken breast without changing the characteristics of the fresh product. The objective of this technology is not to eliminate high concentrations of Salmonella but rather for it to become one of several mitigation approaches that can help, as part of the hurdle technology concept, reducing by at least 1 log the presence of the pathogen. If successful, implementation of this technology in addition to the interventions already applied by the poultry industry can make the product safer for the consumers. We do not have a target temperature as a focus to maintain freshness. However, we understand that temperature is important in maintaining product fresh-like. As temperature increases, proteins will begin to denature and the fresh nature of the product will be impacted. For that reason, we maintain and monitor the product's temperature so it stays below certain levels, but a target temperature is not the focus. Multiple variables are adjusted, and temperature is monitored.

METHODOLOGY

Samples were made by cutting squares of 50 g from chicken breast bought from the supermarket. We evaluated two types of chicken breast, one water-added (water enhanced) and the other one no-water-added. The samples were inoculated with 1 ml of rifampicin resistant (RR) *Salmonella* spp. by pouring the inoculum on the surface. The inoculated samples were assigned to a negative

control (Control), Treatment A (142.7 Kw·s), or Treatment B (124.5 Kw·s). The samples assigned to either of the microwave treatments were treated with a novel six-magnetron microwave. The Control samples were inoculated but did not receive application of microwaves. The samples were then diluted on buffered peptone water (BPW), serial diluted, and plated on tryptic soy agar + rifampicin. After incubation for 24 h at 35 °C, the colony forming units were counted and then transformed to Log_{10} CFU/g. For the results analysis we did an analysis of variance (ANOVA) to know if there was a statistical significance between the treatment and control. The experiment had two replications with independent samples and during two different days. Microwaves were applied at two different energy levels and were fired for 52.5 seconds and 60.0 seconds. The treatment time inside the treatment chamber was approximately 47.6 seconds for both treatments.

RESULTS

We found that both of the microwave treatments were statistically different to the control ($P < 0.05$). The microwave Treatment A was the most effective reducing the concentration of *Salmonella* RR in the inoculated chicken breast by more than 1 Log CFU/50g (> 90% of inoculated microbial population) (Figure 1). We also evaluated two types of chicken breast, water enhanced chicken and non-water-added chicken. Our results demonstrated that there is no effect of the type of chicken on antimicrobial effect of the microwaves (no-interaction of that variable on the treatments) ($P > 0.05$); for that reason, we merged the results of both types of chicken under the same treatment. Furthermore, there was no statistical difference between replications as we expected ($P > 0.05$); this indicates that our results were not obtained by chance.

Figure 1. Comparison of the concentration of *Salmonella* spp. in inoculated chicken samples treated with a novel microwave technology v. control.

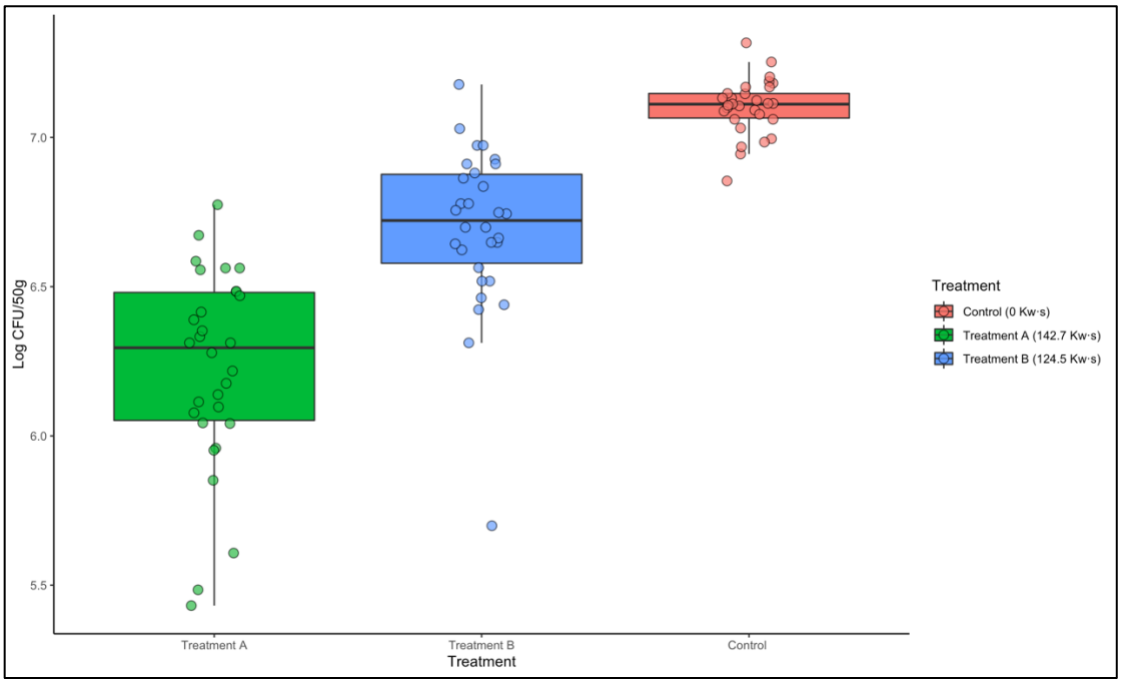

DISCUSSION

Salmonella is normally present in raw chicken at low concentrations; however, in this study we inoculated the samples at 6.81 Log CFU/ml with the objective to have a high concentration of bacteria to observe potential reduction. Furthermore, we understand that this technology would not be used by itself since the poultry industry has many antimicrobial interventions, but it might be able to aid in enhancing the food safety programs if applied as a potential post-packaging intervention. The machine used in this evaluation was located in a BSL-II lab for utilization of inoculated product with dangerous pathogens. The machine is a small scale with lower volumes than what is used in industrial applications. Scale to industrial volumes requires the addition of additional microwave energy. The machine has been successfully scaled from this small version to a larger version by increasing the treatment chamber size and adding additional energy, for instance moving from 6Kw to 48Kw power. The industrial machines utilize entry and exit chokes to allow conveyor belt to move product in a continuous manner. Additional efficiencies were seen in the larger version with increased load versus the smaller version.

REFERENCES

[1]. Golden, C. E., & Mishra, A. (2020). Prevalence of salmonella and campylobacter spp. In alternative and conventionally produced chicken in the United States: A systematic review and meta-analysis. *Journal of Food Protection*, *83*(7), 1181–1197. https://doi.org/10.4315/JFP-19-538

[2]. Jayasena, D. D., Ahn, D. U., Nam, K. C., & Jo, C. (2013). Flavour chemistry of chicken meat: A review. *Asian-Australasian Journal of Animal Sciences*, *26*(5), 732–742. https://doi.org/10.5713/ajas.2012.12619

Multimode Microwave Assisted Comminution of a Sulfide ore: Bench Versus Pilot Scale

John H. Forster[1], Adam E. Olmsted[2], Chris A. Pickles[2], Darryel Boucher[1], and Erin R. Bobicki[1]

[1]University of Toronto, Toronto, Canada
[2]Queen's University, Kingston, Canada

Keywords: microwaves, multimode, comminution, permittivity, frequency, absorption,

INTRODUCTION

The application of microwaves in comminution processes has been ongoing for over thirty years, with benefits demonstrated on both the bench and pilot scale. Comminution, an incredibly energy intensive process, may greatly benefit from innovation leading to a greener mining industry. Microwaves can be applied in the following areas: pre-fracturing, mineral liberation, and ore sorting. Previous research efforts have demonstrated that the phenomenon of microwave heating can be used to exploit the different dielectric properties between valuable and gangue mineral phases. The thermal gradient between the two phases (which have different coefficients of thermal expansion) induces stresses along the grain boundaries leading to the formation of microfractures. Early publications have shown that low-power microwave pre-treatment of ores with long irradiation times can reduce ore competency by up to 70% [1, 2]. It has also been reported that the liberation of valuable minerals can be increased to upwards of 84% [3]. Previous high power tests have investigated the use of monomode field distributions [4], but scale-up remains a constant challenge for such a system. The aim of this paper is to compare microwave assisted grinding on the bench scale versus the pilot scale to demonstrate the great potential of high power multimode microwave systems for the mining industry.

METHODOLOGY

Table 1 shows the ICP elemental analysis of the sulfide ore. The corresponding dielectric properties were measured using the cavity perturbation technique [5] from 24 to 1100°C under a 10 sccm flow of ultra high purity argon. Microwave assisted grinding experiments were performed in parallel on the bench (Microwave Research and Applications; BP-211, 3.2 kW; 2450 MHz) and pilot scale (Thermowave; CMP150; 150 kW; 915 MHz). Each bench microwave test used 50 g of sample (2 to 3.35 mm particle size). Several treated samples were then combined to produce a charge for grinding in a jar mill. For the pilot test, the rocks (25.4 to 63.5 mm in size), were irradiated for several seconds (Figure 2) at high power and ground in a SAG mill. The maximum bulk (bench

samples) and surface (pilot sample) temperatures were measured using a Type-K thermocouple and FLIR infrared camera, respectively. Untreated (UT) samples were ground under the exact same conditions to be able to calculate the reductions in work indices of the microwave treated (MWT) samples. The microwave energy doses and reductions in work indices were compared to determine the effects of scale-up (Table 2).

Table 1. ICP assays of the as-received sulfide ore

Element	Al	Ca	Fe	Mg	S	Si	Zn
wt. (%)	7.70	1.68	4.00	0.88	0.48	28.00	0.64

RESULTS

Figure 1 shows the dielectric property measurements for the two frequency bands relating to the bench scale (2466 MHz) and pilot scale (912 MHz). They follow a similar trend from ambient to the maximum temperature. There is a gradual loss in the real permittivity from ambient up to 100°C. It remains constant up to 450°C before returning to its original value at 500°C. The imaginary permittivity for 912 MHz delineates that of 2466 MHz up to about 450°C, at which point it slowly begins to overtake the 2466 MHz curve.

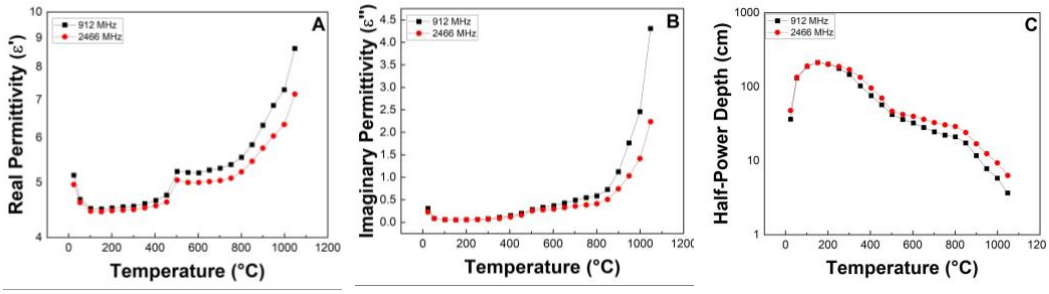

Figure 1. Real (A) and imaginary (B) permittivities, and half-power depth (C) of the sulfide ore.

Table 2. Microwave energy doses, temperatures, and grindability results

Test Description	Microwave Energy Dose (kWh/tonne)	Max. Measured Temperature (°C)	Work Index (kWh/t)	Work Index Reduction (%)
Bench UT	-	-	16.4	-
Bench MWT	4267	283	14.8	9.8
Pilot UT	-	-	12.2	-
Pilot MWT	3	34	10.9	10.7

DISCUSSION

Permittivity measurements of the sulfide ore revealed it to be a relatively low loss material with a moderate dielectric constant, indicating that it would be suitable for high power microwave treatment without arcing. The half-power depth started at 38.2 cm at

24°C, which is larger than the particle size used during processing, meaning that it would be feasible to treat large rocks in the pilot test using microwaves at 915 MHz.

A significant amount of microwave energy was required on the bench scale (measured maximum bulk sample temperature of 283°C), where a reduction of 9.8% was realized after grinding the sample to a P_{80} of 72 μm. For the pilot sample (maximum infrared temperature of 34°C), which was ground to a P_{80} of 1.7 mm, an energy savings of 10.7% was achieved. Despite the fact that the bench and pilot samples obtained similar energy savings during grinding, the required microwave energy dose was several magnitudes lower for the pilot sample. This improvement in energy consumption per tonne of ore is required to economically justify scaling up this technology to an industry level.

In a monomode system a standing wave pattern can be generated for focused destruction of the ore. However, for the size of the applicator, which must be built to meet industry throughputs, a lower microwave frequency band such as 433 MHz is required [6]. This range may not be permitted depending on the country in which the operation is located. Conversely, multimode systems are advantageous in this regard as they can be scaled up without this restriction. While the input energy dose for the pilot sample was more than the reduction in the work index, the overall energy use may be lower due to the improved liberation of the treated sample, which will benefit downstream unit operations.

CONCLUSION

The application of both low and high power multimode microwaves to a sulfide ore resulted in similar reductions in the energy requirements during comminution. However, this was achieved with a much lower energy dose in the pilot test than in the bench scale test. Based on the results obtainted, it is envisioned that optimization of the existing pilot microwave system will result in additional energy savings in comminution.

REFERENCES

[1] J.W. Walkiewicz, A.E. Clark, and S.L. McGill, Microwave-assisted grinding. *IEEE Trans. Ind. Appl.*, vol. 27, pp. 239-243, 1991.

[2] W. Vorster, N.A. Rowson, and S.W. Kingman, The effect of microwave radiation on the processing of Neves Corvo copper ore. *Int. J. Miner Process.*, vol. 63, pp. 29-44, 2001.

[3] O.A. Orumwense, T. Negeri, R. Lastra, Effect of microwave pretreatment on the liberation characteristics of a massive sulfide ore. *Miner. Metall. Proc.*, vol. 21, no 2, pp. 77-85, 2004.

[4] A.R. Batchelor, A.J. Buttress, D.A. Jones, J. Katrib, D. Way, T. Chenje, D. Stoll, C. Dodds, and S.W. Kingman, Towards large scale microwave treatment of ores: part 2-metallurgical testing. *Miner. Eng.*, vol. 111, pp. 5-24, 2017.

[5] R.M. Hutcheon, M.S. De Jong, and F.P. Adams, A system for rapid measurement of rf and microwave properties up to 1400°C. *J. Microwave Power EE*, vol. 27, no 2, pp. 87-92, 1992.

[6] S. Bradshaw, W. Louw, C. Van der Merwe, H. Reader, S. Kingman, M. Celuch, W. Kijewska, Techno-economic considerations in the commercial microwave processing of mineral ores. *J. Microwave Power EE*, vol. 40, no 4, pp. 228-240, 2007.

Alkaline Treatment with Microwave-Assisted of Sugar Cane for Increasing Nutraceutical Properties

María Elena Sánchez-Pardo[1], D. I. Llanes Gil-López[2,3], J. A. Lois-Correa[2]

[1]Instituto Politécnico Nacional, ENCB-Zacatenco, Av. Wilfrido Massieu, 07728, Ciudad de México, México.
[2]Instituto Politécnico Nacional, CICATA-Altamira, km 14.5 carretera Tampico–Puerto Industria Altamira, Tamps., México, 89600
[3]Tecnológico Nacional de México, Instituto Tecnológico de Altamira, Tampico, Tamps.
*Autor correspondencia: M. E. Sánchez Pardo. alimentoselena@hotmail.com

Keywords: antioxidant, fiber, sugar cane bagasse.

INTRODUCTION

Tortilla and its derivatives are one of the fundamental bases of food in Mexico and Latin America. The main component of this food is corn, which is rich in starch and sugars. In recent years, in Mexico and the world, the price of corn has increased ostensibly due to its use in the production of animal feed and biofuels. The process of making a mixed corn-sugarcane bagasse (SCB) flour to produce tortillas, toasts, tortilla chips, and derivatives is presented. It is important to mention that sugarcane bagasse is one of the nine byproducts generated as waste in the production of table sugar from sugarcane. When used as an ingredient in products for human consumption, Bagasse contributes a source of dietary fiber, antioxidants such as polyphenols, and policosanol. The flour was evaluated by confocal laser scanning microscopy (CLSM).

This work aims to develop compound dough for tortillas and derivatives elaborated with mixed corn-bagasse flour of powdered sugarcane, which increases the content of dietary fiber and antioxidants in an important way, with tortillas, tortilla chips, toasts, and derivatives being suitable for human consumption.

In the literature, sugarcane bagasse (SCB) has not previously been used to contribute dietary fiber in corn products for human consumption (1). However, its inclusion in bakery products, such as biscuits, has been reported. As an example, the inclusion of 10% SCB, with acid and alkaline treatments and steam, without considering antioxidants such as policosanol, was reported (2). Policosanol is a mixture of primary aliphatic long-chain alcohols (C_{24} to C_{34}) originally isolated from sugar cane wax (*Saccharum officinarum* L.). The main components of the mixture are octacosanol (60-70%, w / w), triacosanol (10-15%, w / w) and hexacosanol (4-10%, w / w). The antioxidant capacity is determined by the ABTS + radical, which is generated from its precursor 2, 2'-azinobis (3-ethyl

benzothiazoline) -6-sulfonic acid (ABTS) (3). The cationic radical obtained is a stable bluish-green compound with a UV-visible absorption spectrum. An artificial radical does not mimic the *in vivo*. Thermodynamically, compounds that have a lower redox potential than ABTS (0.68V) can reduce it, being able to react with the radical. Many phenolic compounds have a lower potential (4).

This paper presents the process of making a corn-SCB-based mixed flour to make tortillas, toasts, chips, flutes, and derivatives, rich in dietary fiber and antioxidants (patent pending). The SCB is proposed, without treatments with a chemical solution, allowing the preservation of antioxidants such as policosanol. The flour was characterized by confocal scanning laser microscopy (MCLB). The aim is to produce a compound dough for tortilla and derivatives, made with mixed corn flour-SCB powder, with significantly increased dietary fiber and antioxidants in tortillas, chips, toasts, and derivatives, which is suitable for human consumption.

METHODOLOGY

For the first time, an innovative waste treatment was undertaken, using alkaline agents, i.e., sodium hydroxide, combined with microwaves. In this sense, experiments have been carried out with different amounts of the alkaline agent sodium hydroxide (NaOH) to optimize the method, since there are reports of high hygroscopicity of sugarcane bagasse. Experiments were carried out with 30 mL, 45 mL, 60 mL, and 75 mL, respectively equivalent to the concentrations 15, 22.5, 30, 37.5 mmol, using the average power (equivalent to 600 W) of a microwave oven, operating at a frequency of 2400 MHz. The heating of the interstitial water distends the cells and leads to the rupture of the material's glands and receptacles, promoting the breaking of the hemicellulose and lignin bonds.

RESULTS

Table 1. Physical-chemical composition of the tortilla made with corn-SCB dough

Tortilla	**µMol trolox / g dry sample (antioxidant capacity**	**% inhibition ABTS $^{++}$**	**dietary fiber g /100 g**
Corn-SCB	20.63±0.4	22.21 ±0.2	24.8 ±2.3
Corn 100% (control)	10.85 ±0.3	14.87 ±0.13	7.91 ±0.4

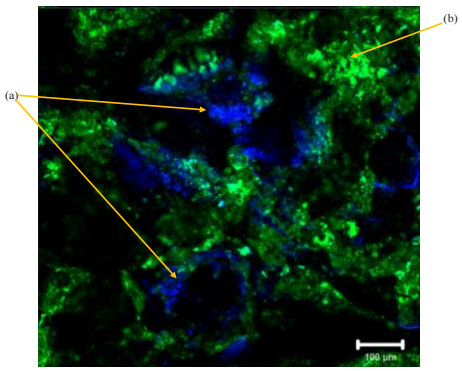

Figure 1. Image of MCLB to tortilla made with dough, with selective calcofluor staining for cellulose, blue (a), and fluorescein for starch (b).

DISCUSSION

Table 1 shows the results of dietary fiber and antioxidant capacity of the tortilla obtained with this process, and it is compared with the traditional tortilla. It is observed that the corn tortilla-BCA has dietary fiber with values of 22-26%, and a traditional tortilla, 7-8%. It should be noted that this increase in dietary fiber is approaching the percentage proposed by the World Health Organization (WHO) of 35 g of dietary fiber per day.

From the CLSM results, a correct interaction (Figure 1) was observed between the starch from corn and the dietary fiber of the SCB, observing starch granules, indicated by (b), surrounded by cellulose, indicated by (a). Using selective staining of calcofluor for cellulose, and fluorescein for starch, a correct incorporation of dietary fiber into the matrix of the tortilla, can be observed, since the spherical and polyhedral shape of the granules are observed in native starches from other sources, surrounded by a cellulose matrix.

CONCLUSION

SCB fibers in human foods, based on corn, provide dietary fiber and antioxidants. Statistically, there is no difference in texture and flavor between the tortilla made with corn flour-SCB and the control product (traditional corn tortilla). An 8% increase in antioxidants was achieved in the formulation with corn flour-SCB. This increase is greater than in similar foods.

REFERENCES

(1) Calleja Pinedo M; Basilia Valenzuela M., 2016. La tortilla como identidad culinaria y producto de consumo global. Región Sociedad. 66, 161-164.
(2) Sangeetha V., Mahadevamma S, Begum, Khyrunnisa and Lakshminarayan, S., 2011. Influence of processed sugarcane bagasse on the microbial, nutritional, rheological and quality characteristics of biscuits. Int. J. Food sci. Nutr. 62, 457-464.
(3) Prior, R. l., Xianli, W., Schaich, K., 2005. Standardized Methods for the Determination of Antioxidant Capacity and Phenolics in Foods and Dietary Supplements. J. Agric. Food Chem., 53, 4290−4302.
(4) Leong, L.P., Shui, G., (2002). An Investigation of Antioxidant Capacity of Fruits in Singapore Markets. Food Chem. 76, 69-75.